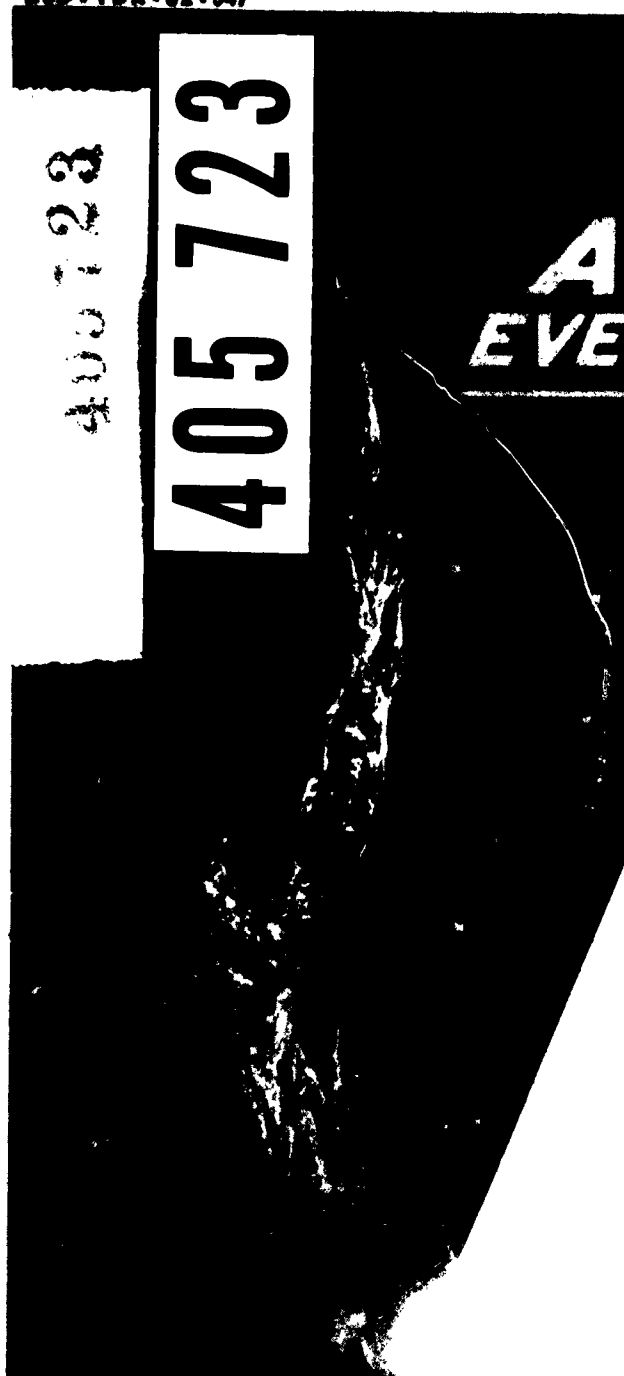

AVCO EVERETT

RESEARCH LABORATORY

a division of
AVCO CORPORATION

THEORY OF STAGNATION-POINT HEAT TRANSFER IN A PARTIALLY IONIZED DIATOMIC GAS

James A. Fay and Nelson H. Kemp

RESEARCH REPORT 144
Contract No. AF 04(694)-33
April 1963

prepared for
HEADQUARTERS
BALLISTIC SYSTEMS DIVISION
AIR FORCE SYSTEMS COMMAND
UNITED STATES AIR FORCE

THEORY OF STAGNATION-POINT HEAT TRANSFER IN A PARTIALLY IONIZED DIATOMIC GAS

by

James A. Fay and Nelson H. Kemp

AVCO-EVERETT RESEARCH LABORATORY
a division of
AVCO CORPORATION
Everett, Massachusetts

Contract No. AF 04(694)-33

April 1963

prepared for

HEADQUARTERS
BALLISTIC SYSTEMS DIVISION
AIR FORCE SYSTEMS COMMAND
UNITED STATES AIR FORCE
Air Force Unit Post Office
Los Angeles 45, California

ABSTRACT

Stagnation-point heat transfer in a partially ionized diatomic gas is considered. The concept of frozen thermal conductivity is used, and a simplified "binary diffusion" model of the gas is proposed. In this model the charge-exchange cross-section for atom-ion collisions is taken to be infinite so there is no relative diffusion of the atoms and the ion-electron pairs. This permits the diffusion effects to be dealt with as if there were only two components, molecules and atom-ion-electron particles, and thus greatly simplifies the calculations. However, the thermodynamic and transport properties are evaluated using all four components, molecules, atoms, ions, and electrons. With this model, calculations are made for both frozen and equilibrium boundary layers in nitrogen up to about 60,000 ft/sec, and arguments are presented for applying the results to air. The results show the equilibrium heat transfer rate to be progressively smaller than the frozen rate as the velocity increases above 30,000 ft/sec, the ratio reaching 2/3 at 50,000 ft/sec. Simple correlation formulas for the results are given.

LIST OF SYMBOLS

A	Constant in the electronic thermal conductivity expression, Eq. (3.22).
a	Stagnation-point velocity gradient.
C_1, C_2	Functions in the equilibrium constants for dissociation and ionization, Eqs. (3.12) and (5.5).
c_{pi}	Specific heat at constant pressure per unit mass of species i.
c_p	Frozen specific heat at constant pressure per unit mass of the mixture.
c_i	Mass fraction of species i.
D_{12}	Binary diffusion coefficient, Eq. (3.14).
$\mathscr{D}$	Diffusion coefficient for binary diffusion model, Eq. (3.18).
D/Dt	Convective derivative operator following the mass-average velocity.
$F_1 - F_8$	Functions of the thermodynamic and transport properties defined in the Appendix.
G	Correlation quantity, Eq. (6.3b).
f	$\int_0^\eta (df/d\eta)\,d\eta$, nondimensional stream function.
f'	$df/d\eta$, normalized velocity, u/u_s.
h_i	Enthalpy per unit mass of species i.
h_i^o	Chemical enthalpy per unit mass of species i.
h	Enthalpy per unit mass of mixture, Eq. (3.8).
h_D^o	Dissociation energy per unit mass of atoms and ions.
h_I^o	Ionization energy per unit mass of ions.
j	Index which is unity for axisymmetric flow and zero for two-dimensional flow.

k_i	Thermal conductivity of species i.
k	Frozen thermal conductivity of mixture.
L	Lewis number, Eq. (3.24).
$\mathcal{L}$	Effective Lewis number, Eq. (6.2).
m_i	Particle mass of species i.
m_{ij}	Reduced mass, $(m_i^{-1} + m_j^{-1})^{-1}$.
$Nu/Re^{1/2}$	Heat transfer parameter based on wall conditions, Eq. (4.14).
n_i	Number density of species i.
n	Number density of mixture.
n_o	Number density of original undissociated molecules, Eq. (3.2).
P^f, P^h P^s, P^θ	Potential functions defined in the Appendix.
p_i	Partial pressure of species i.
p	Pressure of mixture.
Q	Partition function.
q	Energy flux.
R	Gas constant for the molecules, κ/m_M.
r	Radius of axisymmetric body in plane normal to axis.
s	Normalized fraction dissociated, β/β_s.
T	Absolute temperature.
T_D, T_I	Dissociation and ionization temperatures, Eqs. (5.1) and (5.2).
$\underline{V}_i(U_i, V_i)$	Diffusion velocity of species i.
V_∞	Flight velocity, $(2h_s)^{1/2}$.
u, v	Components of mass average velocity.
w_i	Mass rate of formation of species i.
x, y	Distances along and normal to body surface.
Z	Compressibility factor, $p/\rho RT$.

α	Fraction of atoms ionized.
β	Fraction of molecules dissociated.
η	Similarity variable, Eq. (4.6).
θ	Normalized temperature, T/T_s.
κ	Boltzmann's constant.
μ_i	Viscosity of species i.
μ	Viscosity of mixture.
ν_{ij}	Frequency of collision of a species i particle with species j particles.
ρ	Mass density of mixture.
σ	Prandtl number, $c_p \mu/k$.
ϕ	Vibrational contribution to molecule specific heat, Eq. (A.15b).

Subscripts

A	Atom.
D	Dissociation.
E	Electron.
el	Electronic partition function.
I	Ion or ionization.
M	Molecule.
o	Reference condition.
R	Atom-ion-electron particle in binary diffusion model.
r	Rotation.
s	Inviscid stagnation conditions.
v	Vibration.

Superscript

$'$	Corrected for proper wall conditions, Eq. (5.9).

I. INTRODUCTION

The advent of interest in the return to earth of space vehicles has recently stimulated study of atmospheric entry at velocities higher than earth-satellite velocity. As with all high speed atmospheric flight, the heating problem is a major concern and so some attention has been focused on heating at speeds from 26,000 to 40,000 ft/sec or more. While radiative heating increases rapidly with flight speed and can become an important problem at these speeds, the present paper is concerned with convective (or aerodynamic) heating. This subject has been extensively studied at lower speeds in connection with ballistic missile technology and is well in hand. When interest shifts to higher speeds, one must ask whether a simple extrapolation of the lower speed work will suffice or whether there are new physical phenomena which enter whose effects are sufficiently in doubt so the extrapolation is uncertain.

In the case of high speed flight in air at least one new phenomenon does appear, and this is ionization. Figure 1 shows on an altitude-velocity plot the equilibrium stagnation temperature and compressibility factor Z. Also shown is a line for 1% ionization and typical trajectories for lunar and interplanetary vehicles. We see that the lunar vehicle traverses a region of ionization greater than 1%, as would any vehicle whose entry velocity is over 30,000 ft/sec. The presence of electrons in the air may have an important effect on the transport properties which determine the aerodynamic heating. Electrons have high diffusivity which will augment the diffusion of ion-electron pairs to the wall, where the ionization energy may be released during recombination. They may also become dominant transporters of translational energy, and thus enhance the thermal conductivity of the air, also tending to increase the heating. To indicate the amount of

energy invested in ionization, Fig. 2 shows the fractions of the equilibrium stagnation enthalpy of air contributed by thermal energy (translation, rotation, and vibration), dissociation energy and ionization energy, at various flight speeds for stagnation pressure of 1 atmosphere in nitrogen. The increasing importance of the ionized component at high speeds is evident.

A number of investigations of convective heat transfer in partially ionized air at a stagnation point have appeared recently. Adams[1] estimated the heat transfer increase due to ionization in a frozen boundary layer, using a Lewis number of unity for the atoms and two for the ion-electron pairs, with a thermal conductivity proportional to the one-half power of the temperature up to 8,000°K, and the five-halves power above that. He found that up to 45,000 ft/sec there was a maximum increase of 30% above the extrapolation of lower speed theories. Three other investigations[2, 3, 4] have dealt with the equilibrium boundary layer, using the transport properties of Hansen.[5] These are "equilibrium" transport properties in which the contributions of dissociation and ionization are included in the specific heat and thermal conductivity. The results indicate heat transfer rates somewhat less than those found by Adams.[1] Finally, heat transfer in ionized nitrogen has been studied by Scala and Warren[6] and by Pallone and VanTassell,[7] also for thermodynamic equilibrium. Scala uses his own values of nitrogen transport properties as described in Ref. 8, while Pallone and VanTassell use transport properties developed by Yos.[9] Scala finds a very rapid rise in heat transfer above 30,000 ft/sec, leading to values larger by a factor of 2.5 than the other theories at 35,000 ft/sec. Pallone and VanTassell[7] find no such effect, and attribute the differences to different transport properties. Scala uses a charge-exchange cross-section for

$N\text{-}N^+$ collisions which is two orders of magnitude smaller than the one used by Yos, and an $N_2\text{-}N^+$ cross-section one order of magnitude smaller. This has a major effect on the equilibrium thermal conductivity, resulting in Scala's value being one to two orders of magnitude above Yos' value in the range from $10,000^\circ K$ to $20,000^\circ K$.

Experimental data included in Refs. 2, 4, and 6 agree with the respective theories. Only the data of Refs. 2 and 6 extend well above 30,000 ft/sec and they disagree strongly there.

The present theoretical investigation of stagnation point heat transfer was undertaken in conjunction with a companion experimental shock-tube study.[23] It differs from previous work in several respects. First, both frozen and equilibrium boundary layer flow are studied with the same gas model. Frozen flow is important since the high velocity flight regime is at high altitudes where the flow may well be frozen. Second, use is made of the "frozen" specific heat and thermal conductivity definitions in both the frozen and equilibrium cases. Third, a simplified binary diffusion model of an ionized diatomic gas is used to obtain the transport properties. The great simplicity and success of two-component models of air in treating dissociated heat transfer suggested the advantages that would exist if a similar model of ionized gases was possible. Such a model has been developed by making use of the fact that the cross-section for exchange of charge between an atom and its ion is much larger than other kinetic cross-sections. It should be noted, however, that this model still has molecules, atoms, atomic ions, and electrons. It is only binary with respect to diffusion, i.e., the diffusional

velocities of the atoms, ions, and electrons are taken to be equal, with a diffusional mass flux of these species equal and opposite to that of the molecules. With this model, analytic expressions for the transport properties can be derived, avoiding the necessity for elaborate curve fitting.

The binary diffusion model also makes the calculation of a frozen boundary layer of manageable size, since only one diffusion equation must be used. The ultimate test of the accuracy of this model rests on a comparison with experiment and with calculations using more detailed models of ionized gases.

In the present paper, the stagnation-point boundary layer problem for the binary diffusion model is solved in the case of nitrogen, using the most recent estimates of nitrogen transport properties. Some comments are made on the application of these results to air.

In the subsequent sections the boundary layer equations will be presented, the thermodynamic and transport properties of the binary diffusion model have developed, and the calculations and results discussed.

II. BOUNDARY LAYER EQUATIONS

The equations describing the stagnation-point boundary layer in a chemically-reacting gas are well known.[11] The momentum and over-all mass conservation equations are

$$\rho \frac{Du}{Dt} = - \frac{\partial p}{\partial x} + \frac{\partial}{\partial y}\left(\mu \frac{\partial u}{\partial y}\right) , \tag{2.1}$$

$$\frac{\partial}{\partial x}(\rho r^j u) + \frac{\partial}{\partial y}(\rho r^j v) = 0 . \tag{2.2}$$

For each chemical species a mass conservation condition states

$$\frac{\partial}{\partial x}\left[\rho r^j (u + U_i) c_i\right] + \frac{\partial}{\partial y}\left[\rho r^j (v + V_i) c_i\right] = w_i r^j .$$

which upon using Eq. (2.2) and the boundary layer simplifications becomes (since r is a function of x only)

$$\rho \frac{Dc_i}{Dt} + \frac{\partial}{\partial y}(\rho V_i c_i) = w_i . \tag{2.3}$$

Finally, the energy equation for the stagnation-point (where pressure and dissipation terms can be neglected) can be written as

$$\rho \frac{Dh}{Dt} = \frac{\partial}{\partial y}(-q_y) , \tag{2.4}$$

where h is the enthalpy of the mixture, defined by

$$h \equiv \Sigma c_i h_i , \tag{2.5}$$

and q_y is the energy flux vector component normal to the surface given by

$$-q_y = k \frac{\partial T}{\partial y} - \sum \rho c_i V_i h_i \ . \qquad (2.6)$$

The energy flux has two parts. The first is the Fourier heat conduction with k the frozen thermal conductivity, i.e., the thermal conductivity the mixture would possess if no chemical change occurred when a temperature gradient was impressed on it. The second part is the energy flux due to the enthalpy carried by diffusion.

A useful alternative form of the energy equation, in terms of temperature, can be obtained by using the definitions of the component specific heats, c_{pi}, and frozen specific heat of the mixture, c_p:

$$c_{pi} \equiv (\partial h_i / \partial T)_p \ , \quad c_p \equiv \sum c_i c_{pi} \ . \qquad (2.7)$$

When Eq. (2.5) is differentiated, and Eq. (2.7) is used, we find

$$\frac{Dh}{Dt} = \sum h_i \frac{Dc_i}{Dt} + c_p \frac{DT}{Dt} \ . \qquad (2.8)$$

When inserted on the left side of Eq. (2.4), this leads, with Eq. (2.6) to

$$\rho c_p \frac{DT}{Dt} + \rho \sum h_i \frac{Dc_i}{Dt} = \frac{\partial}{\partial y}\left(k \frac{\partial T}{\partial y} - \sum \rho c_i V_i h_i\right). \qquad (2.9)$$

For the equilibrium case the c_i are determined by T (and the constant boundary layer pressure p^*) so Eq. (2.9) is the convenient form of the energy equation. For the frozen case, the c_i are determined by the species mass conservation equations (2.3). When we use them to eliminate the Dc_i/Dt term in Eq. (2.9) we find

$$\rho c_p \frac{DT}{Dt} = \frac{\partial}{\partial y}\left(k \frac{\partial T}{\partial y}\right) - \sum \rho c_i V_i c_{pi} \frac{\partial T}{\partial y} - \sum w_i h_i , \qquad (2.10)$$

which, with $w_i = 0$, is the energy equation we will use for the frozen case.

As pointed out in the Introduction, we will use a binary diffusion model of a diatomic gas, the two species being molecules denoted by subscript M and atom-ion-electron particles which we will denote by subscript R. By making use of the relation

$$\sum \rho c_i V_i = 0$$

the diffusion terms in the energy equations (2.9) and (2.10) for the binary diffusion model may be written

$$\sum \rho c_i V_i c_{pi} = \rho c_R V_R (c_{pR} - c_{pM}), \qquad (2.11a)$$

$$\sum \rho c_i V_i h_i = \rho c_R V_R (h_R - h_M). \qquad (2.11b)$$

---

* We assume that the diatomic gas consists of a single atomic component. When this theory is applied to a mixture such as air, this implies the assumption that the ratio of oxygen to nitrogen is invariant through the boundary layer.

When these relations are inserted into (2.10) with $w_i = 0$, and into (2.9) we have the energy equations appropriate to the binary diffusion model under frozen and equilibrium conditions respectively.

The boundary conditions are:

$$y=0: \quad u=v=0, \quad T=T_w = \text{constant}, \quad c_R=0; \tag{2.12a}$$

$$y\to\infty: \quad u\to u_s = xa, \quad T\to T_s, \quad c_R\to c_{Rs}; \tag{2.12b}$$

where we have taken a fully catalytic wall.

To make use of these equations, we must now specify the thermodynamic and transport properties of the gas. Then the solutions of the equations will provide us with the heat transfer to the wall which is found by evaluating Eq. (2.6) at y = 0.

III. THERMODYNAMIC AND TRANSPORT PROPERTIES

In this section we will give the thermodynamic properties of the ionized gas, explain the physical basis for the binary diffusion model, and give explicit expressions for the transport properties used in the numerical calculations.

Thermodynamic Properties

We are dealing with a mixture of molecules, atoms, atomic ions, and electrons, denoted by subscripts M, A, I, and E respectively. For each component with number density n_i, partial pressure p_i, specific heat c_{pi}, enthalpy h_i and dissociation and ionization enthalpy h_i^o we have

$$p_i = n_i K T \quad , \quad h_i = \int_o^T c_{pi}\, dT + h_i^\bullet \tag{3.1}$$

Let β denote the fraction of molecules dissociated and α the fraction of atoms ionized. Then for n_o molecules in the undissociated state we find

$$n_M = n_o(1-\beta), \quad n_A = 2n_o\beta(1-\alpha), \quad n_I = n_E = 2n_o\beta\alpha. \tag{3.2}$$

The corresponding mass fractions are

$$c_M = 1-\beta, \quad c_A = \beta(1-\alpha), \quad c_I = \beta\alpha, \quad c_E = \beta\alpha m_E/m_A. \tag{3.3}$$

The specific heats are all $5\kappa/2$ per particle except for the molecule which also has an additive rotational contribution of $2\kappa/2$ and a vibrational contribution of $\phi\kappa$. Therefore, the specific heats per unit mass are

$$c_{pM} = \left(\frac{7}{2}+\phi\right)\frac{K}{m_M}, \quad c_{pA} = c_{pI} = \frac{5}{2}\frac{K}{m_A}, \quad c_{pE} = \frac{5}{2}\frac{K}{m_E}$$
$$\phi \equiv (T_v/T)^2 e^{T_v/T}\left(e^{T_v/T}-1\right)^{-2} \tag{3.4}$$

Finally, the dissociation energy per unit mass of the atoms and ions will be called h_D° while the ionization energy per unit mass of the ions is h_I° so the enthalpies per unit mass are

$$h_M = c_{pA}T[0.7 + 0.2\Psi], \quad h_A = c_{pA}T + h_D^\circ, \quad h_E = c_{pE}T,$$
$$h_I = c_{pA}T + h_D^\circ + h_I^\circ, \quad \Psi \equiv (T_v/T)(e^{T_v/T} - 1)^{-1}. \tag{3.5}$$

The properties of the mixture can now be found. By summing the partial pressures the equation of state becomes

$$p = n\kappa T = \rho Z R T, \quad Z \equiv 1 + \beta(1+2\alpha). \tag{3.6}$$

where R is the gas constant for the molecules, κ/m_M. The mixture frozen specific heat is

$$c_p \equiv \sum c_i c_{pi} = c_{pA}\left[(1-\beta)(0.7+0.2\phi) + \beta(1+\alpha)\right], \tag{3.7}$$

and the enthalpy per unit mass is

$$h \equiv \sum c_i h_i = c_p T + \beta(h_D^\circ + \alpha h_I^\circ). \tag{3.8}$$

As mentioned in the Introduction, for diffusion purposes we will consider the gas to be a binary mixture of molecules and atom-ion-electron particles, denoted by subscript R. The mass fraction and specific heat of species R are found from Eqs. (3.3) and (3.4) to be

$$c_R = \beta, \qquad c_{pR} = c_{pA}(1+\alpha), \tag{3.9a}$$

which of course agree with $c_M + c_R = 1$ and $c_M c_{pM} + c_R c_{pR} = c_p$. The corresponding enthalpy is found from Eqs. (3.3), (3.5) and (3.9a) as

$$h_R = c_R^{-1}\left(c_A h_A + c_I h_I + c_E h_E\right)$$
$$= h_A + \alpha\left(h_I - h_A + h_E m_E/m_A\right), \tag{3.9b}$$

which agrees with $c_M h_M + c_R h_R = h$.

The summation term on the left side of the equilibrium energy equation (2.9) is a purely thermodynamic term which represents the reaction contribution to the convection of enthalpy (or reaction specific heat times temperature convection). Using Eqs. (3.3), (3.4), (3.5) and (3.9b) it can be written

$$\sum h_i \frac{Dc_i}{Dt} = (h_R - h_M)\frac{D\beta}{Dt} + (c_{pA}T + h_I^\circ)\frac{D\alpha}{Dt} . \qquad (3.10)$$

When the gas mixture is in thermochemical equilibrium the fractions dissociated and ionized are functions of the pressure and temperature determined by expressions for the equilibrium constants of the reactions

$$A_2 \rightleftarrows 2A , \quad A \rightleftarrows A^+ + E^- .$$

These expressions are found to be

$$\frac{\beta^2(1-\alpha)^2}{1-\beta}\ \frac{C_1(T/T_o)^{-1/2}}{1+\beta(1+2\alpha)} = e^{-T_D/T} , \qquad (3.11a)$$

$$\frac{\beta\alpha^2}{1-\alpha}\ \frac{C_2(T/T_o)^{-5/2}}{1+\beta(1+2\alpha)} = e^{-T_I/T} , \qquad (3.11b)$$

where

$$C_1 \equiv \frac{4\rho T_o^{-1/2}}{K}\left(\frac{h_P}{\pi m_A K}\right)^{3/2} \frac{Q_v Q_r}{T^2}\ \frac{Q_{eM}}{(Q_{eA})^2} , \qquad (3.12)$$

$$C_2 \equiv \frac{2 p T_o^{-5/2}}{K} \left(\frac{h_p^2}{2\pi m_E K} \right)^{3/2} \frac{Q_{e\ell A}}{Q_{e\ell I} Q_{e\ell E}} \qquad (3.12)$$ (Con't)

h_p is Planck's constant

Here T_o is a reference temperature later taken to be the external temperature, T_D and T_I are the dissociation and ionization temperatures respectively, Q_v and Q_r are the vibrational and rotational partition functions of the molecule, and the $Q_{e\ell}$ are the various electronic partition functions. The pressure p is the pressure in the boundary layer, which is the constant stagnation pressure p_s. Since the internal partition functions depend only on temperature, these relations give α and β in the equilibrium boundary layer as functions of temperature alone.

Transport Properties

Our basic approach is to consider the flux of energy to be composed of two parts; the diffusion of translational, rotational and vibrational energy due to a temperature gradient and the flux of dissociation and ionization energy due to concentration gradients, treating each part independently as was previously done in the dissociated air boundary layer.[11] This is in contrast to the method often employed in equilibrium boundary layer calculations which makes use of an "equilibrium" or total thermal conductivity.[5,12-17] The present approach is necessary if nonequilibrium boundary layers are to be considered. It is, of course, still useful in the limiting case of equilibrium, though there it has the disadvantage of requiring specification of the mass fraction of each species present.

In the nonequilibrium case numerical solution of the boundary layer equations for a partially dissociated and ionized gas is complicated

by the necessity of introducing a diffusion equation for each species present. We shall now show that a useful approximation can be made which requires only a single diffusion equation, leading to what we shall call a binary diffusion model.

In Fig. 3 are shown some elastic collision cross-sections for N, N_2, and A. Also shown are charge-exchange cross-sections for A, Xe, and N_2 colliding with their ions. What is readily apparent from these measurements is that the charge-exchange cross-section for the collision of a particle with its ion is nearly a factor of ten higher than the kinetic cross-sections which determine thermal conductivity, viscosity and diffusion coefficients of unlike species. While the important cross-section for the $N\text{-}N^+$ charge-exchange collision has not been measured, an estimate by Yos[9] places it close to that for $A\text{-}A^+$.

In considering the relative diffusion of molecules, atoms, ions and electrons, we would expect the diffusion velocities of the atoms and their ions to be nearly equal, because the large charge-exchange cross-section would make relative motion of the atoms and ions very difficult. Certainly in the limit of infinite charge-exchange cross-section, both atoms and ions would have equal diffusional velocities. Now a similar statement can be made for the diffusional velocities of the ions and electrons, for an ambipolar diffusion of ion-electron pairs will always occur within diffusion layers which are thick compared to the Debye distance. We can then conclude that, in the limit of a charge-exchange cross-section which is very large compared with kinetic cross-sections, the atoms, ions, and electrons will diffuse with equal velocities, and may be considered a single component when determining the particle flux. The molecules then constitute the second

component having an oppositely-directed diffusional velocity. This constitutes the binary diffusion model approximation.

We now proceed to the determination of the diffusional velocity of the atoms, ions, and electrons. In a binary mixture of particles denoted by the subscripts 1 and 2, the difference in diffusion velocities may be related to the gradient of partial pressure by:[18]

$$\nabla p_1 = m_{12}(\underline{V}_2 - \underline{V}_1) n_1 \nu_{12} \tag{3.13}$$

in which m_{12} is the reduced mass, $(m_1^{-1} + m_2^{-1})^{-1}$, and ν_{12} is the frequency of collision of particle 1 with type 2 particles. $n_1\nu_{12}$ is the total collision frequency of unlike particles and is determined by the binary diffusion coefficient, D_{12}:

$$n_1\nu_{12} = n_2\nu_{21} = n_1 n_2 \kappa T/[(n_1+n_2)m_{12}D_{12}] \tag{3.14}$$

The absolute value of the diffusion velocity is determined by the condition of equality of mass flux:

$$n_1 m_1 \underline{V}_1 = -n_2 m_2 \underline{V}_2 \tag{3.15}$$

For a mixture of molecules, atoms, ions and electrons, denoted by subscripts M, A, I, and E respectively, in which the latter three components have the same diffusional velocity, $\underline{V}_R$, we replace Eq.(3.13) by

$$\nabla(p_A + p_I + p_E) = m_{MA}(\underline{V}_M - \underline{V}_R)(n_A\nu_{AM} + n_I\nu_{IM}) \tag{3.16}$$

This expresses the conservation of momentum of the atoms, ions, and electrons: the gradient of the sum of the partial pressures is the rate of gain of momentum of these particles while the term on the right is the rate of loss of momentum by virtue of collisions of atoms and ions with the molecules. (The electrons have negligible average momentum.) The equality of mass flux can then be written as

$$(n_A + n_I) m_A \underline{V}_R = -n_M m_M \underline{V}_M \tag{3.17}$$

An equation corresponding to Eq. (3.14) may be used to define a diffusion coefficient, $\mathcal{D}$, for this binary diffusion model:

$$n_A \nu_{AM} + n_I \nu_{IM} = \frac{(n_A + n_I) n_M K T}{(n_M + n_A + n_I) m_{MA} \mathcal{D}} \tag{3.18}$$

If the ion-molecule and atom-molecule cross-sections are equal, then $\mathcal{D}$ would be the binary diffusion coefficient for atoms (or ions) diffusing through molecules. In the numerical calculations of this paper, this equality has been assumed for simplicity (see Fig. 3).

To obtain an explicit expression for $\underline{V}_R$ from Eq. (3.16), we eliminate $\underline{V}_M$ by means of Eq. (3.17) and the collision frequencies using Eq. (3.18). The result is

$$-\rho \underline{V}_R = \frac{m_M}{KT} \frac{n_M + n_A + n_I}{n_A + n_I} \mathcal{D} \nabla (p_A + p_I + p_E) \tag{3.19}$$

The sum of the partial pressures can be written in terms of the (constant) total pressure p_s and the number densities as

$$p_A + p_I + p_E = \frac{n_A + n_I + n_E}{n} p_s = \frac{2\beta(1+\alpha)}{1+\beta(1+2\alpha)} p_s ,$$

the last step coming from Eqs. (3.2). This is differentiated and inserted in Eq. (3.19). If we use the gas law, Eq. (3.6), the number densities, Eqs. (3.2), and the fact that for the atom-ion-electron species, $c_R = \beta$ according to Eq. (3.9), we may finally write the mass flux of that species as

$$-\rho c_R V_R = \frac{n_M + n_A + n_I}{n} \rho \mathcal{D} \left[(1+\alpha) \nabla\beta + \beta(1-\beta) \nabla\alpha \right] . \tag{3.20}$$

This mass flux equation reduces to the usual ambipolar diffusion formula if we consider the proper limiting case. For a slightly dissociated gas ($\beta \ll 1$) in which all the atoms have been ionized ($\alpha = 1$), the last factor of Eq. (3.20) becomes $2 \nabla\beta$, which is twice the value it would have if the atoms were uncharged. On the other hand, for a completely dissociated but slightly ionized gas ($\beta = 1$, $\alpha \ll 1$), the mass flux given by Eq. (3.20) is exactly zero, rather than the ambipolar value for ions diffusing through atoms. This is a necessary consequence of our assumption as to the importance of charge-exchange in reducing the relative diffusion of ions and atoms to a value which is small compared with other transport effects. It should be noted, therefore, that Eq. (3.20) is not generally applicable to the ambipolar diffusion of ions through atoms.

We turn next to a determination of the thermal conductivity of the mixture of molecules, atoms, ions, and electrons. While there are several empirical rules for determining the thermal conductivity of mixtures,[10,19,20] we will adopt the following simple approach. First, the contribution of the

ions to the thermal conductivity is smaller than that of the electrons by a factor equal to the square root of the ratio of electron mass to ion mass, and hence will be neglected. Secondly, the thermal conductivity of the entire mixture will be assumed to be the sum of the thermal conductivities of the electrons, as determined by Spitzer[21] for a singly ionized plasma, and the thermal conductivity of an atom-molecule mixture, as calculated by Yun et al,[22] for N_2-N mixtures.* The latter may be suitably approximated by:

$$k_{MA} = k_A (0.72 + 1.28\beta)/(1+\beta),$$

$$k_A = 8.4 \times 10^{-7} T^{0.81} \quad \text{cal/sec-cm-}^\circ\text{K} . \tag{3.21}$$

which gives the correct value for pure N_2 ($\beta = 0$) at 300°K. The electron thermal conductivity, k_E, is shown in Fig. 4 and was approximated by

$$k_E = AT^{2.16}, \tag{3.22}$$

where A was determined by the electron density, n_E, in the free stream.** Hence, the total thermal conductivity, k, becomes:

$$k = k_{MA} + k_E . \tag{3.23}$$

---

* A more exact calculation, using the method described in Ref. 10, showed that this approximation is accurate for α greater than a few percent.

** The temperature dependence of k_E is somewhat less than $T^{2.5}$ because of the logarithmic term in the coulomb cross-section.

As used in the calculations, the diffusivity, $\mathcal{D}$, is made dimensionless by dividing by the thermal diffusivity, $k/\rho c_p$, of a pure atomic gas at the same heavy particle density, $n_M + n_A + n_I$, and temperature as the mixture, to give a Lewis number L, of:

$$L \equiv (n_M + n_A + n_I)\, \mathcal{D}\, m_A\, c_{pA}/k_A \,. \tag{3.24}$$

According to the discussion following Eq. (3.18), $\mathcal{D}$ is the atom-molecule binary diffusion coefficient and from the calculations of Yun et al[22] L was found to be 0.6 for $10^3 < T < 10^4$. Using this definition of L, the diffusive mass flux, Eq. (3.20) becomes

$$-\rho c_R \underline{V}_R = \frac{2L}{Z} \frac{k_A}{c_{pA}} \left[(1+\alpha)\nabla\beta + \beta(1-\beta)\nabla\alpha\right], \tag{3.25}$$

in which the factor 2/Z is the ratio of the average particle mass ρ/n to the atomic mass.

The viscosity of the mixture is relatively unimportant in determining the heat transfer, and appears in the boundary layer equations only in the form of the Prandtl number, σ, in the momentum equation. To estimate the viscosity, we first assume that the ions contribute nothing because of their large coulomb cross-section, so that the viscosity is equal to the mole fraction of atoms and molecules times the viscosity of an atom-molecule mixture having the relative proportions as found in the gas. Using the numerical results of Yun et al[22] this becomes:

$$\mu = \frac{0.82 + 1.18\beta}{1+\beta} \left[\frac{1+\beta-2\alpha\beta}{1+\beta+2\alpha\beta}\right] \mu_A \,, \tag{3.26}$$

in which μ_A is the viscosity of the pure atomic gas and the term in brackets is the mole fraction of atoms and molecules. Next, we assume that the temperature dependence of μ_A and k_A are identical, so that

$$\sigma \equiv \frac{c_p \mu}{k} = \frac{2}{3}\left(\frac{0.82+1.18\beta}{1+\beta}\right)\left(\frac{1+\beta-2\alpha\beta}{1+\beta+2\alpha\beta}\right)\frac{c_p}{c_{pA}}\frac{k_A}{k}, \qquad (3.27)$$

in which the Prandtl number of an atomic gas is taken as 2/3.

While this expression for σ is reasonably accurate at high temperatures, it gives the incorrect value of 0.531 at a cold wall ($T_w = 300^\circ K$, $\alpha = \beta = 0$). This is the result of our simplifying assumption of Eq. (3.21) that the ratio of atomic to molecular thermal conductivity is independent of temperature. Since it has been shown that the heat transfer is principally dependent upon the transport properties in the free stream and only slightly affected by the values of these properties at the wall, this inaccuracy of σ_w and μ_w will have a negligible effect upon the calculated heat transfer. On the other hand, to form the heat transfer parameter, $Nu/Re^{1/2}$, from the calculated heat transfer one must use the correct values of σ_w and μ_w. This correction is discussed in Section V.

Finally, we apply the binary diffusion approximation to the diffusion Eq. (2.3) for atoms and for ions, in a frozen boundary layer. Using Eqs. (3.3) for the mass fractions and putting the same diffusion velocity for both species, we find

$$\rho \frac{D\beta(1-\alpha)}{Dt} + \frac{\partial}{\partial y}\left[\rho V_R \beta(1-\alpha)\right] = 0, \qquad (3.28)$$

$$\rho \frac{D\beta\alpha}{Dt} + \frac{\partial}{\partial y}\left[\rho V_R \beta\right] = 0. \tag{3.29}$$

Addition gives the equation for the atom-ion-electron mass fraction $c_R = \beta$ as

$$\rho \frac{D\beta}{Dt} + \frac{\partial}{\partial y}\left(\rho V_R \beta\right) = 0. \tag{3.30}$$

With the help of this relation we reduce Eq. (3.29) to

$$\rho\beta\left[\frac{D\alpha}{Dt} + V_R \frac{\partial \alpha}{\partial y}\right] = 0, \tag{3.31}$$

which determines the fraction of atoms ionized, α. However, the quantity in square brackets is just the derivative of α following a diffusing atom-ion-electron particle, so the equation states that α is constant following this particle. Since all particles come from the edge of the boundary layer where $\alpha = \alpha_s$, we conclude that in the frozen boundary layer, $\alpha = \alpha_s$ = constant.

IV. TRANSFORMATION OF EQUATIONS

By making use of Eq. (2.11a) for the summation term and Eq. (3.25) for the diffusion velocity V_R, the diffusion equation for species R and the energy equation for frozen flow, Eqs. (3.30) and (2.10) with $w_i = 0$, can be written

$$\rho \frac{D\beta}{Dt} - \frac{\partial}{\partial y}\left[(1+\alpha_s)\frac{2L}{Z}\frac{\rho_A}{c_{pA}}\frac{\partial \beta}{\partial y}\right] = 0, \tag{4.1}$$

$$\rho c_p \frac{DT}{Dt} = \frac{\partial}{\partial y}\left(k\frac{\partial T}{\partial y}\right) + \frac{c_{pR}-c_{pM}}{c_{pA}}(1+\alpha_s)\frac{2L}{Z}\rho_A \frac{\partial \beta}{\partial y}\frac{\partial T}{\partial y}. \tag{4.2}$$

Here α has been put equal to α_s and $\nabla \alpha = 0$, in accord with the deduction from Eq. (3.31). The corresponding momentum and total mass conservation relations are Eqs. (2.1) and (2.2), repeated here with the pressure term replaced by its external value in terms of the external velocity u_s and density ρ_s:

$$\rho \frac{Du}{Dt} = \rho_s \frac{du_s}{dx} + \frac{\partial}{\partial y}\left(\mu \frac{\partial u}{\partial y}\right), \tag{4.3}$$

$$\frac{\partial}{\partial x}(\rho x^j u) + \frac{\partial}{\partial y}(\rho x^j v) = 0. \tag{4.4}$$

The cylindrical radius r of the body has been taken as x since we are considering the vicinity of the stagnation-point.

For equilibrium flow the energy equation is obtained from Eq. (2.9), again using Eq. (3.25) in the summation terms from Eqs. (2.11b) and (3.10). In addition, we recognize that both α and β are given functions of T, so

that grad $\beta = (d\beta/dT)$ grad T and similarly for α. Then the energy equation for equilibrium becomes

$$\rho\left[c_p \frac{DT}{Dt} + (h_R - h_M)\frac{d\beta}{dT}\frac{DT}{Dt} + (c_{pA}T + h_I^\circ)\beta\frac{D\alpha}{Dt}\right]$$
$$= \frac{\partial}{\partial y}\left\{k\frac{\partial T}{\partial y} + (h_R - h_M)\frac{2L}{Z}\frac{k_A}{c_{pA}}\left[(1+\alpha)\frac{d\beta}{dT} + \beta(1-\beta)\frac{d\alpha}{dT}\right]\frac{\partial T}{\partial y}\right\}. \tag{4.5}$$

Since exact similarity holds at a stagnation-point, we can now reduce these partial differential equations to ordinary differential equations in the stagnation-point similarity variable

$$\eta \equiv \left[\frac{(1+j)a\,c_{p_o}}{\rho_o k_o}\right]^{1/2}\int_o^y \rho\, dy\ , \tag{4.6}$$

where the subscript o refers to a constant reference condition and a is the stagnation-point velocity gradient u_s/x. Normalized dependent variables are defined as

$$T/T_s = \Theta(\eta)\ , \quad u/u_s = df(\eta)/d\eta\ , \quad \beta/\beta_s = s(\eta), \tag{4.7}$$

and are all taken to be functions of η, in accord with the existence of similar solutions. The inviscid stagnation-point quantities T_s and β_s are constant but the velocity $u_s = ax$ as mentioned above.

When v is eliminated from the convective derivative operator D/Dt by use of (4.4), the diffusion, energy, and momentum conservation Eqs. (4.1)-(4.3) and (4.5) become

$$\frac{d}{d\eta}\left[\frac{k_A\rho}{k_o\rho_o}(1+\alpha_s)\frac{2L}{Z}\frac{c_{p_o}}{c_{pA}}\frac{ds}{d\eta}\right] + f\frac{ds}{d\eta} = 0, \tag{4.8}$$

$$\frac{d}{d\eta}\left(\frac{k\rho}{k_0\rho_0}\frac{d\theta}{d\eta}\right) + \frac{c_p}{c_{p0}}\frac{d\theta}{d\eta}\left[f + \frac{k_A\rho}{k_0\rho_0}(1+\alpha_s)\frac{2L}{Z}\frac{c_{p0}}{c_{pA}}\frac{c_{pR}-c_{pM}}{c_p}\beta_s\frac{ds}{d\eta}\right] = 0, \tag{4.9}$$

$$\frac{d}{d\eta}\left(\frac{k\rho/c_p}{k_0\rho_0/c_{p0}}\sigma\frac{d^2f}{d\eta^2}\right) + f\frac{d^2f}{d\eta^2} + \frac{1}{1+j}\left[\frac{\rho_s}{\rho_0} - \left(\frac{df}{d\eta}\right)^2\right] = 0, \tag{4.10}$$

where $\sigma = c_p\mu/k$, and

$$\frac{d}{d\eta}\left\{\frac{k\rho}{k_0\rho_0}\frac{d\theta}{d\eta} + \frac{k_A\rho}{k_0\rho_0}\frac{2L}{Z}\frac{h_R-h_M}{c_{pA}T_s}\left[(1+\alpha)\frac{d\beta}{d\theta} + \beta(1-\beta)\frac{d\alpha}{d\theta}\right]\frac{d\theta}{d\eta}\right\}$$
$$+ \frac{c_p}{c_{p0}}f\left[\frac{d\theta}{d\eta} + \frac{h_R-h_M}{c_pT_s}\frac{d\beta}{d\theta}\frac{d\theta}{d\eta} + \frac{c_{pA}T_s\theta + h_I^\circ}{c_pT_s}\beta\frac{d\alpha}{d\theta}\frac{d\theta}{d\eta}\right] = 0. \tag{4.11}$$

The corresponding form for the boundary conditions is found from Eqs. (2.12) as

$$\eta = 0: \quad f = df/d\eta = 0, \quad \theta = \theta_w = \text{constant}, \quad s = 0; \tag{4.12a}$$

$$\eta \to \infty: \quad df/d\eta \to 1, \quad \theta \to 1, \quad s \to 1. \tag{4.12b}$$

For the frozen case, Eqs. (4.8), (4.9), and (4.10) are to be solved for f, θ, and s. For the equilibrium case, α and β are both determined by T from thermodynamic considerations, as also pointed out in Section III, and the two variables f and θ are found from Eqs. (4.10) and (4.11). In this latter case, the boundary conditions on s in Eqs. (4.12) may be ignored.

The variable η defined in Eq. (4.6) and used here differs from

the usual variable, such as that of Fay and Riddell,[11] by a factor $\sigma_o^{1/2}$, and the same is true of our function f. The present definitions result in the appearance of the Prandtl number σ in the momentum Eq. (4.10) instead of the energy Eqs. (4.9) or (4.11), and reflect our choice of ρk rather than the more usual $\rho\mu$ as the basic combination of fluid properties. Since the heat transfer rate rather than the shear stress is of primary interest here, it seems more suitable to relegate the only appearance of viscosity, which is in σ, to the momentum equation which is known to be weakly coupled to the energy equation. This simplifies the difficult task of calculating the viscosity of ionized gases, since a rough approximation will suffice in the momentum equation. The frequent use of $\rho\mu$ as basic is a holdover from the incompressible point of view that the velocity profile could be found first and the temperature profile calculated afterwards, and seems inappropriate to the present-day emphasis on heat transfer rather than shear stress. For the case of constant Prandtl number $\sigma = \sigma_o$, the present equations can be put into their more familiar form by replacing η and f by $\sigma_o^{1/2}\eta$ and $\sigma_o^{1/2} f$.

The heat transfer rate at the wall is found by evaluating Eq. (2.6), which is also the quantity in the square bracket on the right side of Eq. (4.5) in the binary diffusion model. The transformed version of this is in the square bracket of the first term on the right of Eq. (4.11) except for some cancelled constants. When they are restored, the wall heat transfer becomes, for frozen and equilibrium respectively,

$$-q_w = \left[(1+j)\, a\, c_{p_o} k_o \rho_o\right]^{1/2} T_s \times \left[\frac{k\rho}{k_o\rho_o}\frac{d\theta}{d\eta} + \frac{k_{eA}\rho}{k_o\rho_o}\frac{2L}{Z}\frac{h_R - h_M}{c_{pA}T_s}(1+\alpha_s)\beta_s\frac{ds}{d\eta}\right]_w \qquad (4.13a)$$

$$-q_w = \left[(1+j)\,a\,c_{p_0}\,k_0\,\rho_0\right]^{1/2} T_s \left\{ \frac{k\rho}{k_0\rho_0}\frac{d\theta}{d\eta} + \frac{k_A\rho}{k_0\rho_0}\frac{2L}{Z}\frac{h_R - h_M}{c_{p_A}T_s}\left[(1+\alpha)\frac{d\beta}{d\theta} + \beta(1-\beta)\frac{d\alpha}{d\theta}\right]\frac{d\theta}{d\eta}\right\}_w \tag{4.13b}$$

The thermodynamic and transport properties which appear in Eqs. (4.8)-(4.13) are given in Section III as functions of α, β, and T, and complete the relations necessary to solve the differential equations and find the heat transfer rate $-q_w$. A suitable nondimensional heat transfer parameter is obtained by introducing the Nusselt and Reynolds numbers based on wall conditions by

$$\frac{Nu}{\sqrt{Re}} \equiv \frac{(-q_w)\,x\,c_{pw}}{k_w\,(h_s - h_w)}\left(\frac{\rho_w u_s x}{\mu_w}\right)^{-1/2} = \frac{(-q_w)}{h_s - h_w}\left(\frac{\sigma_w c_{pw}}{k_w \rho_w a}\right)^{1/2} \tag{4.14}$$

For numerical integration, the differential equations are put in a form in which the fluid properties do not have to be differentiated. The transformation to this form, together with expressions for the thermodynamic and transport properties as they are used in the calculations, is given in the Appendix.

V. CALCULATIONS

Calculations were made for both equilibrium and frozen boundary layers, using the physical constants of nitrogen, which has a dissociation energy of 9.756 electron volts per molecule, and an ionization energy of 14.48 electron volts per atom. These lead to the following values of the dissociation and ionization constants:

$$T_D \equiv h_D^\circ/R = 113{,}200\,^\circ K, \quad T_I \equiv h_I^\circ/2R = 168{,}100\,^\circ K \tag{5.1}$$

$$\frac{h_D^\circ}{c_{pA}} = 0.2\,T_D = 22{,}640\,^\circ K, \quad \frac{h_I^\circ}{c_{pA}} = 0.4\,T_I = 67{,}200\,^\circ K \tag{5.2}$$

The rotational and vibrational temperatures of nitrogen are

$$T_r = 2.90\,^\circ K, \quad T_v = 3400\,^\circ K \tag{5.3}$$

so the rotational partition function may be approximated by its asymptotic value $Q_r = T/2T_r$. The vibrational partition function is $Q_v = [\,1 - \exp(-T_v/T)]^{-1}$ while for the electronic partition functions we take

$$Q_{elM} = 1, \quad Q_{elA} = 4, \quad Q_{elI} = 9, \quad Q_{elE} = 2 \tag{5.4}$$

Then the functions C_1 and C_2 of Eqs. (3.12) become

$$C_1 = \frac{0.260 \times 10^{-10}\,\rho_s T_s^{-1/2}}{(\theta/\theta_v)(1 - e^{-\theta_v/\theta})}, \quad C_2 = 1.33\,\rho_s T_s^{-5/2} \tag{5.5}$$

where p_s is in dynes/cm^2 and T_s is in ^oK.

The Lewis number L was defined in Eq. (3.24) and its value discussed immediately following that equation. We concluded that for nitrogen, the best estimate for L is 0.6, and this is the value we used for most of the calculations. However, in order to see the effect of possible uncertainties in L, some calculations were made for L = 0.3 and L = 1.0.

All the calculations were done for an axisymmetric boundary layer so we used

$$j = 1, \tag{5.6}$$

and in all cases the wall temperature was taken to be

$$T_w = 300^\circ K. \tag{5.7}$$

Equilibrium Boundary Layer

For equilibrium external flow, the calculations were performed by choosing values of j, T_w, T_s and p_s. Then α_s and β_s could be determined from Eqs. (A.32) and (A.31). The equation of state, Eq. (3.6) then yielded a value of ρ_s, which combined with α_s to give an external electron density n_{Es}. From Fig. 4 a value of A corresponding to this n_{Es} was chosen. When combined with the nitrogen constants given above, this procedure yielded all the necessary input information for the solution of Eqs. (A.21)-(A.25), which was done by guessing P_w^h and P_w^f and iterating.

Frozen Boundary Layer

The same procedure as for the equilibrium boundary layer was followed in the case of a frozen boundary layer with equilibrium external flow to determine the values of α_s, β_s, and A. Of course, in this case,

α is constant at the value α_s and $\beta = \beta_s s$ is determined by a differential equation instead of an algebraic one. The input information was used to solve Eq. (A.1)-(A.7) iteratively by guessing P_w^θ, P_w^f, and P_w^s.

Results

The results of the calculations were expressed in terms of the heat transfer parameter by use of Eqs. (A.10) and (A.28). As pointed out in Section III the viscosity and Prandtl number used in the calculations are in error at low temperatures. A corrected heat transfer parameter was computed using correct transport properties at $T_w = 300^\circ K$. If we denote the corrected quantities by a prime, Eq. (4.14) shows that

$$\frac{Nu/Re^{1/2}}{(\sigma_w c_{pw}/k_w)^{1/2}} = \frac{(Nu/Re^{1/2})'}{\sigma_w'/(\mu_w')^{1/2}} . \tag{5.8}$$

The properties on the left were found by the formulas of the present paper while those on the right were taken as $\sigma_w' = 0.713$, $\mu_w' = 0.179 \times 10^{-3}$ g/cm-sec for $T_w = 300^\circ K$. The corrected heat transfer parameter for a $300^\circ K$ wall is then related to the one actually calculated from Eqs. (A.10) and (A.28) by

$$(Nu/Re^{1/2})' = 1.14\,(Nu/Re^{1/2}) . \tag{5.9}$$

Calculations were performed for a wall temperature T_w of $300^\circ K$, and for a range of stagnation temperatures at four values of p_s: 10^2, 10, 1 and 10^{-2} atmospheres. The results are given in Table I.

In Fig. 5 the corrected heat transfer parameter from Eq. (5.9) is plotted against a flight velocity V_∞ obtained by equating the stagnation enthalpy to $V_\infty^2/2$, i.e.,

$$V_\infty \equiv (2h_s)^{1/2} . \qquad (5.10)$$

Also included in Fig. 5 are the air and nitrogen calculations of Pallone and Van Tassell,[7] the air calculations of Cohen[3] and Hoshizaki,[2] and the nitrogen calculations of Scala and Warren.[6] All these calculations are for equilibrium air or nitrogen and all except Cohen's below 29,100 ft/sec use the equilibrium thermal conductivity and specific heat.

In the present calculations, the equilibrium case also involves the equilibrium thermal conductivity and specific heat, though we do not separate them as such. Inspection of the equilibrium energy equation (4.11) shows that if the factor $(\rho/k_o\rho_o)\,(d\theta/d\eta)$ is factored out of the curly bracket, what remains is the equilibrium thermal conductivity. Similarly, the second term of Eq. (4.11) yields the equilibrium specific heat as the coefficient of $(f/c_{po})\,(d\theta/d\eta)$. These expressions are calculated during the course of the boundary layer solutions and can be compared with expressions given by others for the same quantities. A good standard of comparison for nitrogen is the recent set of properties given by Yos[9], who used the most recent data to make an accurate calculation of transport properties. When such a comparison is made for equilibrium specific heat good agreement is found between our values and his.* Fairly good agreement is also obtained with the air values of Hansen,[5] except for a bump at 3500°K due to oxygen dissociation. Such agreement is not surprising since equilibrium specific

* Ref. 9 does not contain values of equilibrium specific heat, which were kindly provided in a private communication.

heat is a purely thermodynamic quantity. A more interesting comparison is shown in Fig. 6, where the equilibrium thermal conductivity of Yos for N_2 and Hansen for air are shown, together with the results of the present $L = 0.6$ calculations, all for $p_s = 1$ atm. It can be seen that the agreement between the nitrogen conductivity of Yos and the present values are excellent. This is particularly significant because the equilibrium thermal conductivity involves the use of the binary diffusion model in the present formulation. The agreement between our results and those of Yos in Fig. 6 lend considerable support to this simple model in cases where the charge-exchange cross-section is an order of magnitude bigger than the kinetic cross-sections for unlike species. The air conductivity of Hansen differs considerably from the nitrogen values, both at low temperatures, where the effect of oxygen makes itself felt, and at the higher temperatures where air should behave much like nitrogen. Most of this latter difference is attributable, not to any real difference between air and nitrogen, but to the more up-to-date cross-section information used by Yos. This can be seen by comparing the equilibrium thermal conductivity for air also given by Yos in Ref. 9, with Hansen's values. Except at low temperatures, Yos' air values are very close to his nitrogen values, and so deviate considerably from those of Hansen.

VI. CORRELATION FORMULAS

The major uncertainty in the calculations presented here lies in the inexact knowledge of the transport properties. If the results of such calculations can be correlated in terms of the input data, then moderate changes in future estimates of the transport properties will not require a recalculation of the boundary layer solution. This procedure, which was used by Fay and Riddell,[11] makes it possible to differentiate between the effects due to the assumed numerical values of the transport properties and those resulting from the assumptions as to the physical processes which are important. In this section, we shall discuss such a correlation. In addition, for practical calculation of heat transfer to hypersonic vehicles, it is most convenient for the heat transfer to be expressed as a function of flight conditions rather than transport property data. Since the heat transfer is primarily a function of stagnation conditions, we also will give a correlation formula which makes use of our transport property estimates but which explicitly involves flight velocity and stagnation density and pressure, it being assumed that the latter may be readily determined from the flight conditions.

To determine a suitable form for a transport property correlation which will account for a variation in L, we rewrite the wall heat transfer rate, which is the quantity in curly brackets on the right

side of Eq. (4.5) evaluated at the wall. By using $dh_M = c_{pM}dT$ we find

$$-q_w = \frac{k_w}{c_{pw}} \left\{ \frac{\partial h_M}{\partial y} + \left(\frac{2L}{Z} \frac{k_A}{k} \frac{c_{pM}}{c_{pA}} \right) (h_R - h_M) \left[\frac{\partial}{\partial y} (1+\alpha)\beta - \beta^2 \frac{\partial \alpha}{\partial y} \right] \right\}_w , \quad (6.1)$$

in which the term involving α and β has been rearranged so that the first term varies monotonically throughout the entire boundary layer and the second term is zero in a frozen boundary layer. Defining an effective Lewis number, $\mathcal{L}$, in terms of stagnation conditions by

$$\mathcal{L} \equiv \left(\frac{2L}{Z} \frac{k_A}{k} \frac{c_{pM}}{c_{pA}} \right)_s , \quad (6.2)$$

we would expect the heat transfer to be proportional to the integral of Eq. (6.1), except for the exponent of $\mathcal{L}$:

$$\frac{Nu}{Re^{1/2}} \propto \left[\frac{h_{Ms}}{h_s} + \mathcal{L}^n \left(1 - \frac{h_{Ms}}{h_s} \right) \left\{ \begin{matrix} 1 + \alpha_s (1 - \beta_s) \\ 1 + \alpha_s \end{matrix} \right\} \right] \quad (6.3a)$$

Here the upper and lower terms in the curly bracket refer to equilibrium and frozen flow, respectively, and we have made use of the fact that $(h_R - h_M)\beta = h - h_M$. (Notice that in actuality the quantity $1 + \alpha_s (1 - \beta_s)$ is always very close to unity in the equilibrium case, and we took it to be so.) The form of Eq. (6.3a) is similar to that used in Ref. 11, where n was found to be 0.52 for equilibrium and 0.63 for frozen flow.

We have found that, if n = 0.6, and we define

$$G \equiv \frac{h_{Ns}}{h_s} + \mathcal{L}^{0.6}\left(1 - \frac{h_{Ns}}{h_s}\right)\left\{\frac{1}{1+\alpha_s}\right\}, \qquad (6.3b)$$

the quantity $(Nu/\sqrt{Re})'/G$ correlates within ± 7% for $0.3 < L < 1.0$ and for both frozen and equilibrium flow at fixed stagnation conditions. These values are given in Table I and plotted against $(\rho k/c_p)_s/(\rho k/c_p)_w$ in Fig. 8. Unlike the correlation of Ref. 11, however, the variation of $(Nu/\sqrt{Re})'/G$ with varying stagnation conditions could not be correlated as a function of the $\rho k/c_p$ ratio alone, but was found to depend somewhat upon stagnation pressure level also, as shown in Fig. 8. The final correlation can be expressed as

$$\frac{(Nu/Re^{1/2})'}{G} = 0.58\left[\frac{(\rho k/c_p)_s}{(\rho k/c_p)_w}\right]^{-m}, \qquad (6.4)$$

$$m = 0.015 + 0.009(\log p_s) + 0.071(\log p_s)^2 + 0.045(\log p_s)^3,$$

where $\log p_s$ is the logarithm to the base 10 of the stagnation pressure in atmospheres. This formula holds within ± 10% for $\beta_s > 0.4$. The analogous line from Ref. 11, Eq. (58), is also given in Fig. 8, and we see that points with no significant amount of ionization fit that line quite well.

The difference between the correlation of Ref. 11, and Eq. (6.4) above deserves some comment. The calculations of Ref. 11 were carried out for only a few selected stagnation conditions with dissociation less than 60% and no effect of ionization, but over a wide range of wall

temperatures. In the present calculations, the wall temperature has been held fixed while the stagnation pressure has been varied by a factor of 10^4, and we ranged from 12% dissociated to 94% ionized. It is therefore our opinion that the correlation shown in Fig. 8 is indicative of the effect of the variation of stagnation pressure (and hence composition), while that of Ref. 11 reflects the effect of variation of wall temperature for fixed stagnation conditions. Since the heat transfer to cold walls is only slightly affected by wall temperature, the present correlation is more significant than that of Ref. 11 for the problem at hand.

A correlation in terms of flight conditions is given in Fig. 9, which is a plot of $(Nu/\sqrt{Re})'$ against flight velocity for L = 0.6 and various stagnation pressures. The correlation formulas are:

Equilibrium:
$$(Nu/Re^{1/2})' = 0.47 \qquad 10 < V_\infty < 24$$
$$= 0.47\,(V_\infty/24)^{-N} \qquad 24 < V_\infty < 60, \qquad (6.5a)$$
$$N = 0.83 - 0.11(\log p_s) - 0.02(\log p_s)^2,$$

Frozen:
$$(Nu/Re^{1/2})' = 0.47 \qquad 10 < V_\infty < 24$$
$$= 0.47\,(V_\infty/24)^{-0.83} \qquad 24 < V_\infty < 34 \qquad (6.5b)$$
$$= 0.35 \qquad 34 < V_\infty < 60,$$

where V_∞ is in kilofeet per second and $\log p_s$ is the logarithm to the base 10 of the stagnation pressure in atmospheres. This correlation is accurate to ± 9%. These formulas are related to the wall heat transfer

rate by Eq. (4.14). For a 300°K wall, with the stagnation-point velocity gradient a taken as the Newtonian value $(2\, p_s/\rho_s)^{1/2}$ and $h_s - h_w = V_\infty^2/2$, this becomes

$$-q_w = \frac{6.00 \times 10^2}{\sqrt{R_N}} \left(\frac{Nu}{Re^{1/2}}\right)' p_s^{1/2} \left(\frac{V_\infty}{24}\right)^2 \left(\frac{\rho_s}{\rho_s}\right)^{1/4} \frac{BTU}{ft^2\text{-}sec} \,. \qquad (6.6)$$

Here R_N is the nose radius of curvature in feet, V_∞ is again measured in kilofeet per second and p_s and ρ_s are measured in atmospheres and amagats (1.29×10^{-3} gm/cm^3 or 2.45×10^{-3} slug/ft^3) respectively.

rate by Eq. (4.14). For a 300°K wall, with the stagnation-point velocity gradient a taken as the Newtonian value $(2\, p_s/\rho_s)^{1/2}$ and $h_s - h_w = V_\infty^2/2$, this becomes

$$-q_w = \frac{6.00 \times 10^2}{\sqrt{R_N}} \left(\frac{Nu}{Re^{1/2}}\right)' p_s^{1/2} \left(\frac{V_\infty}{24}\right)^2 \left(\frac{\rho_s}{\rho_s}\right)^{1/4} \frac{BTU}{ft^2\text{-}sec} \,. \qquad (6.6)$$

Here R_N is the nose radius of curvature in feet, V_∞ is again measured in kilofeet per second and p_s and ρ_s are measured in atmospheres and amagats (1.29×10^{-3} gm/cm^3 or 2.45×10^{-3} slug/ft^3) respectively.

VII. DISCUSSION

The results of the present theory show a marked difference between the equilibrium and frozen boundary layer heat transfers in the ionized region (V_∞ > 30 kiloft/sec), the latter being greater than the former as the velocity increases. This difference can be directly related to the diffusive flux of atoms, ions, and electrons as given by Eq. (3.25). While in the frozen boundary layer, $\nabla\alpha = 0$ and $\nabla\beta$ is finite throughout the boundary layer, in the equilibrium boundary layer $\beta = 1$ through the ionized portion of the boundary layer, with the result that there is no diffusional mass flux in this region of those species which can carry ionization and dissociation energy to the wall. In other words, there is mass diffusion only where there is a changing mass fraction of molecules, which occurs throughout the frozen boundary layer but only near the wall for the equilibrium boundary layer.

This result is in marked contrast to that for the dissociated gas boundary layer, in which the heat transfer for frozen and equilibrium boundary layers are nearly identical even for a Lewis number different from unity.[11] This lack of dependence of the heat transfer on chemical kinetics follows from the binary nature of the dissociated mixture, and would apply equally well to a partially ionized monatomic gas. In the equilibrium ionized diatomic gas boundary layer, however, there is a layer of atoms which separates the molecules at the wall from the ions in the free stream, so that with respect to composition it is primarily a ternary mixture. This can be seen in Fig. 7, where the mass fractions of the various species are plotted for both frozen and equilibrium flow at p_s = 1 atm, T_s = 16,000°K,

L = 0.6. Because of the large charge-exchange cross-section, this atomic layer acts as an insulator, preventing ion-electron pairs from diffusing toward the wall and thereby preventing the transport of ionization energy. This insulating layer is absent in the frozen boundary layer, as seen in Fig. 6, thereby permitting a higher heat transfer rate. One would expect a similar effect in multiply-ionized monatomic gases.

The size of the numerical difference shown in Fig. 5 between the frozen and equilibrium cases is undoubtedly influenced by the assumption of infinite charge-exchange cross-section in the binary diffusion model. However, as long as this cross-section is as large as it is presently thought to be, more exact calculations should show a similar effect, though perhaps not so large in magnitude.

When compared with the equilibrium N_2 calculations of Pallone and Van Tassell[7] at the same pressure (p_s = 1 atm), our results differ at the most by a few percent at the highest velocities. This is not surprising, in view of the previous discussion of the good agreement in equilibrium specific heat and thermal conductivity between our calculations and those of Yos[9] used by Pallone and VanTassell. It confirms that the simple binary diffusion model can be used for accurate prediction of the heating rate in ionized diatomic gases.

Adams[1] has estimated the increase in heat transfer due to ionization in a frozen boundary layer by making use of the correlation formulae of Fay and Riddell[11] together with assumptions as to the effective Lewis numbers for atomic and ambipolar diffusion. According to Fay,[10] Adams' estimate results in a nearly constant value of 0.4 for

$(Nu/\sqrt{Re})'$ for flight velocities between 30 and 45 kilofeet/sec, which is only about 10% above our frozen boundary layer calculation. This is probably due to his choice of unity for L instead of the more realistic value of 0.6.

When compared with the calculations of Scala and Warren for equilibrium N_2, our results (as well as those of Pallone and VanTassell) show major disagreement in the ionized gas region. The difference is undoubtedly due to the very small charge-exchange cross-section assumed by Scala and Warren, as discussed in the Introduction, and for which we can find no physical justification.

The differences in heat transfer between air and nitrogen at the same flight velocity and density ought to be quite small, at least in the ionized region. For a given stagnation enthalpy and pressure in air, the temperature and composition are determined. For an equal stagnation enthalpy in nitrogen, but somewhat different (usually lower) pressure, an equal temperature and hence approximately equal enthalpy of dissociation and ionization can be found. For these corresponding flight conditions, the heat transfer parameters in air and nitrogen ought to be very nearly the same. In view of the fact that the heat transfer parameter in N_2 is determined mostly by flight velocity, being less affected by pressure (or density), we can expect that the heat transfer parameters in air and nitrogen are practically the same at identical flight conditions. But Fig. 5 shows that the equilibrium air calculations of Hoshizaki[2] and Cohen[3] differ to some extent from our equilibrium nitrogen calculations, which seems to contradict this expectation. However, both those investigations used Hansen's[5] air

properties, and as discussed in connection with Fig. 6, his equilibrium thermal conductivity is considerably different from more recent estimates[9] for both air and nitrogen, while ours is in agreement with these estimates. We feel that the differences between Hoshizaki's and Cohen's air calculations and our nitrogen results are mostly attributable to this difference in transport property estimates, rather than any real difference in heat transfer rate between equilibrium air and equilibrium nitrogen.

The present analysis of stagnation-point heat transfer in an ionized diatomic gas has been limited to two cases: either complete thermodynamic equilibrium throughout the boundary layer or frozen atomic and ionic recombination. In both cases the calculations have been done for equilibrium conditions at the edge of the boundary layer, and fully catalytic wall conditions. There are a number of other non-equilibrium effects which have not been considered, such as finite recombination rate processes, unequal electron and heavy particle temperature, the presence of an appreciable concentration of molecular ions, vibrational heat capacity lag, radiative effects, and non-equilibrium conditions at the edge of the boundary layer. These effects, some or all of which may be important, will require more complex models than the one proposed.

VIII. CONCLUSIONS

1) Under the assumption that the atom-ion charge-exchange cross-section is much larger than other cross-sections, it is possible to treat the boundary layer in a dissociated and ionized diatomic gas as a binary mixture for the purposes of determining the diffusive mass fluxes.

2) Both equilibrium and frozen boundary layers may be treated with equal ease through use of this model.

3) The results of our equilibrium boundary layer calculations for N_2 are in good agreement with other calculations using the equilibrium thermal conductivity method and essentially the same transport properties.

4) Heat transfer in a frozen boundary layer is greater than that in an equilibrium boundary layer, the difference increasing with velocity above 30 kilofeet/sec.

ACKNOWLEDGMENT

We are especially indebted to William Nelson for performing the machine calculations with thoroughness and energy.

This research was supported by Headquarters, Ballistic Systems Division, U. S. Air Force, under Contract AF 04(694)-33.

REFERENCES

1. Adams, M.C., "A Look at the Heat Transfer Problem at Super-Satellite Speeds," American Rocket Society, Paper No. 1556-60, Dec.1960. Also published as Avco-Everett Research Laboratory AMP 53, Dec. 1960.

2. Hoshizaki, H., "Heat Transfer in Planetary Atmospheres at Super-Satellite Speeds," ARS Journal, Vol. 32, No.10, pp.1544-1551, Oct. 1962.

3. Cohen, N., "Boundary Layer Similar Solutions and Correlation Equations for Laminar Heat Transfer Distribution in Equilibrium Air at Velocities up to 41,000 Feet per Second," NASA Technical Report R-118, 1961.

4. Pallone, A. and VanTassell, W., "Stagnation Point Heat Transfer for Air in the Ionization Regime," ARS Journal, Vol. 32, No. 3, pp. 436-437, March 1962.

5. Hansen, C.F., "Approximations for the Thermodynamic and Transport Properties of High Temperature Air," NASA Technical Report R-50, 1959, (Supersedes NASA TN 4150.)

6. Scala, S.M. and Warren, W.R., "Hypervelocity Stagnation Point Heat Transfer," ARS Journal, Vol. 32, No.1, pp. 101-102, January 1962

7. Pallone, A. and VanTassell, W., "The Effects of Ionization on Stagnation-Point Heat Transfer in Air and Nitrogen," Avco Corporation Research and Advanced Development Division Technical Memorandum RAD TM-62-75, September 1962.

8. Scala, S. M., "Heating Problems of Re-entry into Planetary Atmospheres from Supercircular Orbiting Velocities," Proceedings of Symposium on Aerothermoelasticity, ASD Technical Report No. 61-645, pp. 552-563, October 1961.

9. Yos, J. M., "Transport Properties of Nitrogen, Hydrogen, Oxygen, and Air to 30,000°K," Avco Corporation Research and Advanced Development Division Technical Memorandum RAD-TM-63-7, March 1963.

10. Fay, J. A., "Hypersonic Heat Transfer in the Air Laminar Boundary Layer," AGARD Hypersonic Specialists Conference, April 1962. Published as Avco-Everett Research Laboratory AMP 71, March 1962.

11. Fay, J. A. and Riddell, F. R., "Theory of Stagnation Point Heat Transfer in Dissociated Air," J. Aeronautical Sciences, Vol. 25, No. 2, pp. 73-85, February 1958.

12. Butler, J. N. and Brokaw, R. S., "Thermal Conductivity of Gas Mixtures in Chemical Equilibrium," J. Chemical Physics, Vol. 26, No. 6, pp. 1636-1643, June 1957.

13. Brokaw, R. S., "Thermal Conductivity of Gas Mixtures in Chemical Equilibrium II," J. Chemical Physics, Vol. 32, No. 4, pp. 1005-1006, April 1960.

14. Bauer, E. and Zlotnick, M., "Transport Coefficients of Air to 8000°K," ARS Journal, Vol. 29, No. 10, Part 1, pp. 721-728, October 1959.

15. Peng, T-C and Pindroh, A. L., "An Improved Calculation of Gas Properties at High Temperatures - Air," American Rocket Society Paper 1995-61. Published in "Magnetohydrodynamics," Proceedings of the Fourth Biennial Gas Dynamics Symposium, Northwestern University Press, Evanston, Illinois, 1962.

16. Burhorn, F., "Berechnung and Messung der Warmeleitfahigkeit von Stickstoff bis 13,000°K," Zeitschrift, für Physik, Vol. 155, No. 1, pp. 42-58. 6 May 1959.

17. Stupochenko, E., Dotsenko, B., Stakhanov, I. and Samuilov, E., "Method of Calculation of the Transport Coefficients of Air at High Temperatures," Fizicheskaya Gazodinamika, USSR Acad. of Sciences, pp. 39-58, translated in ARS Journal, Vol. 30, No. 4, pp. 394-402, April 1960.

18. Chapman, S. and Cowling, T., "The Mathematical Theory of Non-Uniform Gases," Cambridge University Press, Cambridge, England, 1953.

19. Mason, E. A. and Saxena, S. C., "Approximate Formula for the Thermal Conductivity of Gas Mixtures," Physics of Fluids, Vol. 1, No. 5, pp. 361-369, September-October 1958.

20. Mason, E.A. and VonUbisch, H., "Thermal Conductivities of Rare Gas Mixtures," Physics of Fluids, Vol. 3, No. 3, pp. 355-361, May-June 1960.

21. Spitzer, L., "Physics of Fully Ionized Gases," Interscience Publishers, New York, 1956.

22. Yun, K-S., Weissman, S., and Mason, E.A., "High-Temperature Transport Properties of Dissociating Nitrogen and Dissociating Oxygen," Physics of Fluids, Vol. 5, No. 6, pp. 672-678, June 1962.

23. Rose, P.H. and Stankevics, J.O., "Stagnation Point Heat Transfer Measurements in Partially Ionized Air," Research Report 143, Avco-Everett Research Laboratory, April 1963.

APPENDIX

To put the differential equations in final form for numerical calculation, we change the dependent variables in order to avoid having to differentiate the fluid properties. It is convenient to consider the frozen and equilibrium cases separately.

Frozen Boundary Layer

We introduce the variables, P^s, P^θ, f, and P^f by the definitions

$$P^s \equiv F_2^{-1} \frac{ds}{d\eta}, \quad F_2^{-1} \equiv \frac{h_A \rho}{h_0 \rho} (1+\alpha_s) \frac{2L}{Z} \frac{c_{p0}}{c_{pA}} \tag{A.1}$$

$$P^\theta \equiv F_1^{-1} \frac{d\theta}{d\eta}, \quad F_1^{-1} \equiv \frac{h_2 \rho}{h_0 \rho_0} \tag{A.2}$$

$$f' \equiv df/d\eta \tag{A.3}$$

$$P^f \equiv \sigma F_3^{-1} \frac{df'}{d\eta}, \quad F_3^{-1} \equiv \frac{h_2 \rho / c_p}{h_0 \rho_0 / c_{p0}} \tag{A.4}$$

Then the governing differential Eqs. (4.8)-(4.10) become

$$\frac{dP^s}{d\eta} = -F_2 f P^s \tag{A.5}$$

$$\frac{dP^\theta}{d\eta} = -F_3 P^\theta (f + F_4 P^s), \quad F_4 \equiv \frac{\beta_s (c_{pR} - c_{pM})}{c_p} \tag{A.6}$$

$$\frac{dP^f}{d\eta} = -\frac{F_3}{\sigma} f P^f - \frac{1}{1+j}\left[F_5 - (f')^2\right], \quad F_5 \equiv \frac{\rho_s}{\rho} \tag{A.7}$$

This is a system of seven first order equations for the seven unknowns P^s, P^θ, f', P^f, θ, s, f, and the corresponding boundary conditions from Eqs. (4.12) are

$$\eta = 0: \quad f = f' = 0, \quad \theta = \theta_w, \quad s = 0 \tag{A.9a}$$

$$\eta \to \infty: \quad f' \to 1, \quad \theta \to 1, \quad s \to 1 \tag{A.9b}$$

The nondimensional heat transfer parameter of Eq. (4.14) is written by using Eq. (4.13a) for $(-q_w)$ and the definitions (A.1), (A.2), and (A.4):

$$\frac{Nu}{\sqrt{Re}} = \frac{c_{p0} T_s}{h_s - h_w}\left[(1+j)\sigma_w F_{3w}\right]^{1/2}\left[P^\theta_w + \beta_s \frac{c_{pA}}{c_{p0}} F_{7w} P^s_w\right] \tag{A.10}$$

where

$$F_7 \equiv (h_R - h_M)/(c_{pA} T_s) \tag{A.11}$$

The F functions can be expressed in terms of the actual variables of the problem by using the results of Section III. We chose to take the reference conditions as external so subscript zero becomes subscript s. The quantities appearing in the F functions can then be written:

$$\frac{k}{k_A} = \frac{A T_s^{2.16} \theta^{2.16}}{8.4\times10^{-7} T_s^{0.81} \theta^{0.81}} + \frac{0.72 + 1.28\beta}{1+\beta} \qquad \text{(A. 12)}$$

$$\rho/\rho_s = Z_s/Z\theta, \qquad Z = 1 + (1+2\alpha)\beta \qquad \text{(A. 13), (A. 14)}$$

$$c_p/c_{pA} = (1-\beta)(0.7 + 0.2\phi) + \beta(1+\alpha) \qquad \text{(A. 15a)}$$

$$\phi = (\theta_v/\theta)^2 e^{\theta_v/\theta} \left(e^{\theta_v/\theta} - 1\right)^{-2} \qquad \text{(A. 15b)}$$

$$\frac{k}{k_s} = \frac{A T_s^{2.16} \theta^{2.16} + \left(\frac{0.72 + 1.28\beta}{1+\beta}\right) 8.4\times10^{-7} T_s^{0.81} \theta^{0.81}}{A T_s^{2.16} + \left(\frac{0.72 + 1.28\beta_s}{1+\beta_s}\right) 8.4\times10^{-7} T_s^{0.81}} \qquad \text{(A. 16)}$$

$$\sigma = \frac{2}{3} \frac{c_p}{c_{pA}} \frac{k_A}{k} \frac{0.82 + 1.18\beta}{1+\beta} \frac{1 + (1-2\alpha)\beta}{1 + (1+2\alpha)\beta} \qquad \text{(A. 17)}$$

$$\frac{c_{pR} - c_{pM}}{c_{pA}} = 1 + \alpha - (0.7 + 0.2\phi) \qquad \text{(A. 18)}$$

$$\frac{h_R - h_M}{c_{pA} T_s} = \left[1 + \alpha - (0.7 + 0.2\Psi)\right]\theta + \frac{h_D^\circ + \alpha h_I^\circ}{c_{pA} T_s} \qquad \text{(A. 19a)}$$

$$\Psi = (\theta_v/\theta)\left(e^{\theta_v/\theta} - 1\right)^{-1} \qquad \text{(A. 19b)}$$

$$\frac{h_s - h_w}{c_{pA} T_s} = (1-\beta_s)(0.7 + 0.2\psi_s) + (1+\alpha_s)\beta_s + \frac{h_D^\bullet + \alpha_s h_I^\bullet}{c_{pA} T_s}\beta_s - (0.7 + 0.2\psi_w) \qquad \text{(A. 20)}$$

In the frozen case, $\alpha = \alpha_s$ and $\beta = \beta_s$ s in all these expressions.

Equilibrium Boundary Layer

Here we define the variables

$$P^h \equiv F_1^{-1} \frac{d\theta}{d\eta}\left[1 + F_6 F_7\right], \qquad F_1^{-1} \equiv \frac{h_2 \rho}{h_{20} \rho_0}, \qquad \text{(A. 21)}$$

$$F_6 \equiv \frac{h_{2A}}{h_2}\frac{2L}{Z}\left[(1+\alpha)\frac{d\beta}{d\theta} + \beta(1-\beta)\frac{d\alpha}{d\theta}\right], \quad F_7 \equiv \frac{h_R - h_H}{c_{pA} T_s}, \qquad \text{(A. 22)}$$

$$f' \equiv df/d\eta, \qquad \text{(A. 23)}$$

$$P^f \equiv \sigma F_3^{-1}\frac{df'}{d\eta}, \qquad F_3^{-1} \equiv \frac{h_2 \rho / c_p}{h_{20} \rho_0 / c_{p0}}. \qquad \text{(A. 24)}$$

We then find for the governing differential equations

$$\frac{dP^h}{d\eta} = -\frac{F_3 f P^h}{1 + F_6 F_7}\left[1 + \frac{c_{pA}}{c_p}\left(F_7 \frac{d\beta}{d\theta} + F_8 \beta \frac{d\alpha}{d\theta}\right)\right], \qquad \text{(A. 25)}$$

$$F_8 \equiv \theta + h_I^\bullet / c_{pA} T_s,$$

$$\frac{dP^f}{d\eta} = -\frac{F_3}{\sigma} f P^f - \frac{1}{1+j}\left[F_5 - (f')^2\right], \quad F_5 \equiv \frac{\rho_s}{\rho}. \qquad \text{(A. 26)}$$

These are five first order equations for the five variables P^h, f', P^f, θ, f, and the boundary conditions are

$$\eta = 0: \quad f = f' = 0, \quad \theta = \theta_w ; \tag{A.27a}$$

$$\eta \to \infty: \quad f' \to 1, \quad \theta \to 1. \tag{A.27b}$$

The heat transfer parameter is again obtained by inserting Eq. (4.13b) into Eq. (4.14). This time, using definition (A.21), we find

$$\frac{Nu}{Re^{1/2}} = \frac{c_{p0} T_s}{h_s - h_w} \left[(1+j)\, \sigma_w F_{3w} \right]^{1/2} P_w^{k} . \tag{A.28}$$

All the quantities appearing in the new functions, F_6 and F_8 are already defined in Eqs. (A.12)-(A.20), except α and β as functions of θ. From Eqs. (3.11) and (3.12) of Section III, the relations between α, β, and θ are

$$\frac{\beta^2 (1-\alpha)^2}{1-\beta} \; \frac{C_1 \theta^{-1/2}}{1+\beta(1+2\alpha)} = e^{-\theta_D/\theta}, \quad C_1 = \frac{0.260 \times 10^{-10} \rho_s T_s^{-1/2}}{(\theta/\theta_v)(1 - e^{\theta_v/\theta})} , \tag{A.29}$$

$$\frac{\alpha^2 \beta}{1-\alpha} \; \frac{C_2 \theta^{-5/2}}{1+\beta(1+2\alpha)} = e^{-\theta_I/\theta}, \quad C_2 = 1.33\, \rho_s T_s^{-5/2}, \tag{A.30}$$

where p_s is in dynes/cm^2 and T_s in $^\circ$K. If Eq. (A.30) is solved for β we find

$$\beta^{-1} = \frac{\alpha^2}{1-\alpha} C_2 \theta^{-5/2} e^{\theta_I/\theta} - (1+2\alpha) . \tag{A.31}$$

When this is inserted into the ratio of Eqs. (A.29) and (A.30), the following quartic equation for α as a function of θ results:

$$\alpha^4\left(C_2\theta^{-5/2}e^{\theta_I/\theta}+2\right) - (1-\alpha)^4 C_1 C_2^{-1}\theta^2 e^{-(\theta_I-\theta_b)/\theta} - 2\alpha^2 = 0 \qquad \text{(A.32)}$$

By using Descarte's rule of signs on the equation obtained from this one by letting $\alpha = (1+\alpha')^{-1}$ one can show that there is one real value of α in the interval $0 < \alpha < 1$, in accord with physical reality. When this root is obtained for a given θ, substitution into Eq. (A.31) gives the appropriate β.

The derivatives $d\alpha/d\theta$ and $d\beta/d\theta$ which appear in Eq. (A.22) can be found as a function of α, β, and θ by combining the θ derivatives of Eqs. (A.31) and (A.32).

TABLE I - RESULTS OF CALCULATIONS (T_w = 300°K)

p_s(atm)	T_s(°K)	L	a_s	β_s	A x 10^{12}	$h_s/c_{pA}T_s$	V_∞ (10^3ft/sec)	$(\rho k/c_p)_s / (\rho k/c_p)_w$	Equil. $(Nu/\sqrt{Re})'$	Frozen $(Nu/\sqrt{Re})'$	Equil. $(Nu/\sqrt{Re})' G^{-1}$	Frozen $(Nu/\sqrt{Re})' G^{-1}$
10^2	19,000	0.6	3.09×10^{-1}	0.9985	4.74	3.59	46.6	0.555	0.338	---	0.793	---
10^2	22,000	0.6	5.80×10^{-1}	0.9998	4.95	4.38	55.5	0.448	0.293	0.363	0.810	0.794
10	10,000	0.6	8.86×10^{-3}	0.895	2.49	3.07	31.4	0.449	0.401	---	0.620	---
10	13,000	0.6	8.43×10^{-2}	0.9939	3.14	3.25	36.7	0.469	0.366	---	0.655	---
10	16,000	0.6	3.42×10^{-1}	1	3.56	4.19	46.2	0.377	0.304	---	0.680	---
10	19,000	0.6	7.16×10^{-1}	1	3.72	5.44	57.5	0.270	0.240	0.349	0.680	0.709
1	2,000	0.6	0	0	0	0.776	7.05	0.569	0.531	0.530	0.531	0.530
1	4,000	0.6	0	0.001	0	0.832	10.3	0.482	0.480	---	0.480	---
1	6,000	0.6	3.69×10^{-5}	0.117	1.23	1.31	15.9	0.527	0.485	0.484	0.485	0.487
1	8,000	0.3	2.68×10^{-3}	0.810	1.79	3.29	29.0	0.397	0.330	0.298	0.590	0.534
1	8,000	0.6	2.68×10^{-3}	0.810	1.79	3.29	29.0	0.397	0.410	0.399	0.579	0.564
1	8,000	1.0	2.68×10^{-3}	0.810	1.79	3.29	29.0	0.397	0.501	0.505	0.577	0.580
1	10,000	0.3	2.73×10^{-2}	0.988	2.20	3.44	33.2	0.392	0.301	0.280	0.601	0.553
1	10,000	0.6	2.73×10^{-2}	0.988	2.20	3.44	33.2	0.392	0.375	0.376	0.598	0.591
1	10,000	1.0	2.73×10^{-2}	0.988	2.20	3.44	33.2	0.392	0.461	0.476	0.605	0.612
1	13,000	0.6	2.58×10^{-1}	0.9997	2.67	4.33	42.4	0.318	0.306	0.362	0.616	0.642
1	16,000	0.3	7.55×10^{-1}	1	2.85	6.34	56.9	0.191	0.178	0.243	0.601	0.589
1	16,000	0.6	7.55×10^{-1}	1	2.85	6.34	56.9	0.191	0.218	0.347	0.581	0.625
1	16,000	1.0	7.55×10^{-1}	1	2.85	6.34	56.9	0.191	0.266	0.455	0.575	0.645
10^{-2}	2,000	0.6	0	0	0	0.776	7.05	0.569	0.530	---	0.530	---
10^{-2}	5,500	0.6	1.67×10^{-4}	0.438	1.13	2.72	21.8	0.429	0.460	---	0.524	---
10^{-2}	6,000	0.6	1.82×10^{-4}	0.763	1.15	3.84	27.1	0.364	0.419	0.413	0.555	0.546
10^{-2}	8,000	0.6	2.54×10^{-2}	0.9976	1.49	4.07	32.2	0.328	0.372	0.378	0.560	0.560
10^{-2}	10,000	0.6	2.63×10^{-1}	1	1.73	5.29	41.1	0.236	0.296	0.365	0.534	0.555
10^{-2}	13,000	0.6	9.36×10^{-1}	1	1.82	8.51	59.5	0.112	0.179	0.349	0.450	0.519

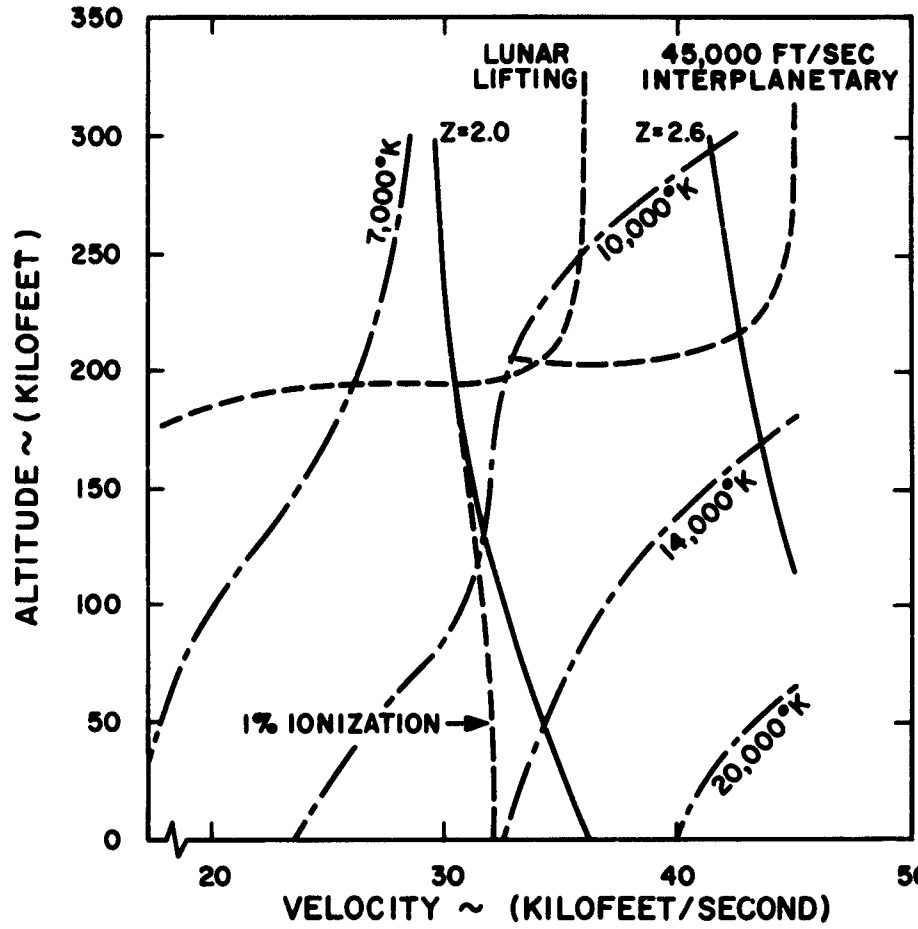

Fig. 1 - Equilibrium stagnation temperature and compressibility factor Z as a function of velocity and altitude. Typical trajectories for lunar and interplanetary vehicles are also shown.

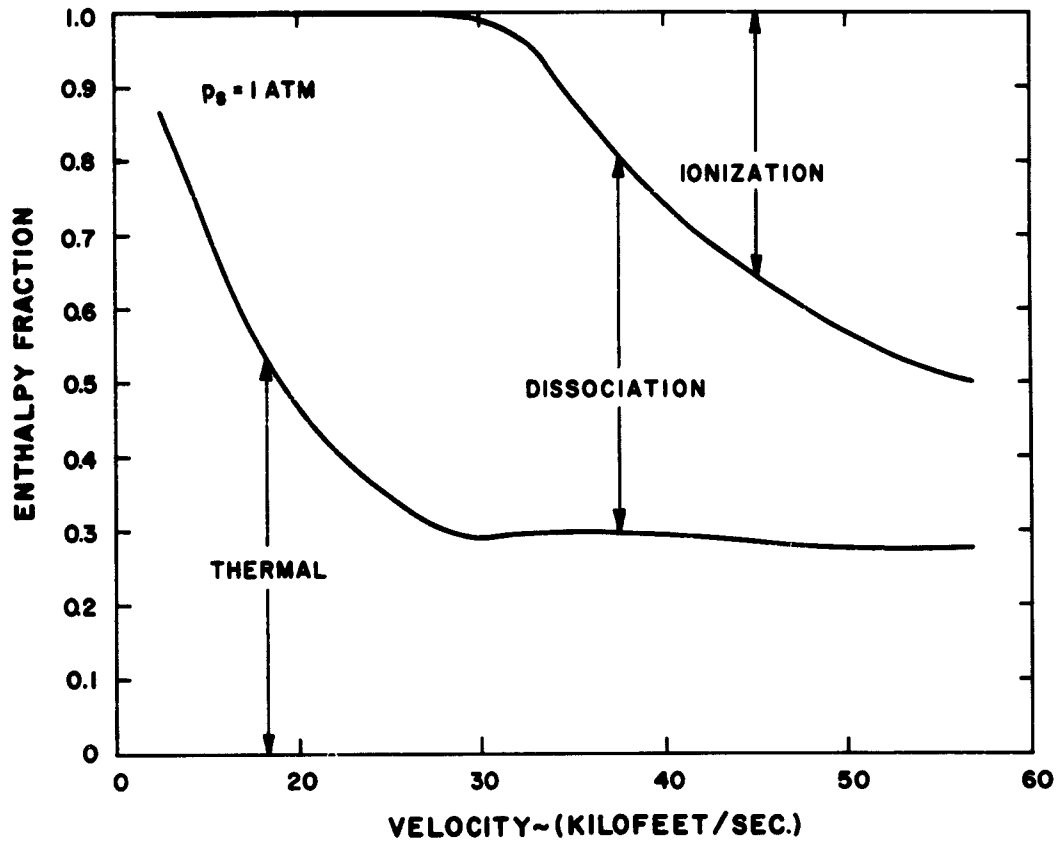

Fig. 2 - Fractional distribution of equilibrium stagnation enthalpy among thermal, dissociative and ionic modes for nitrogen at a pressure of one atmosphere.

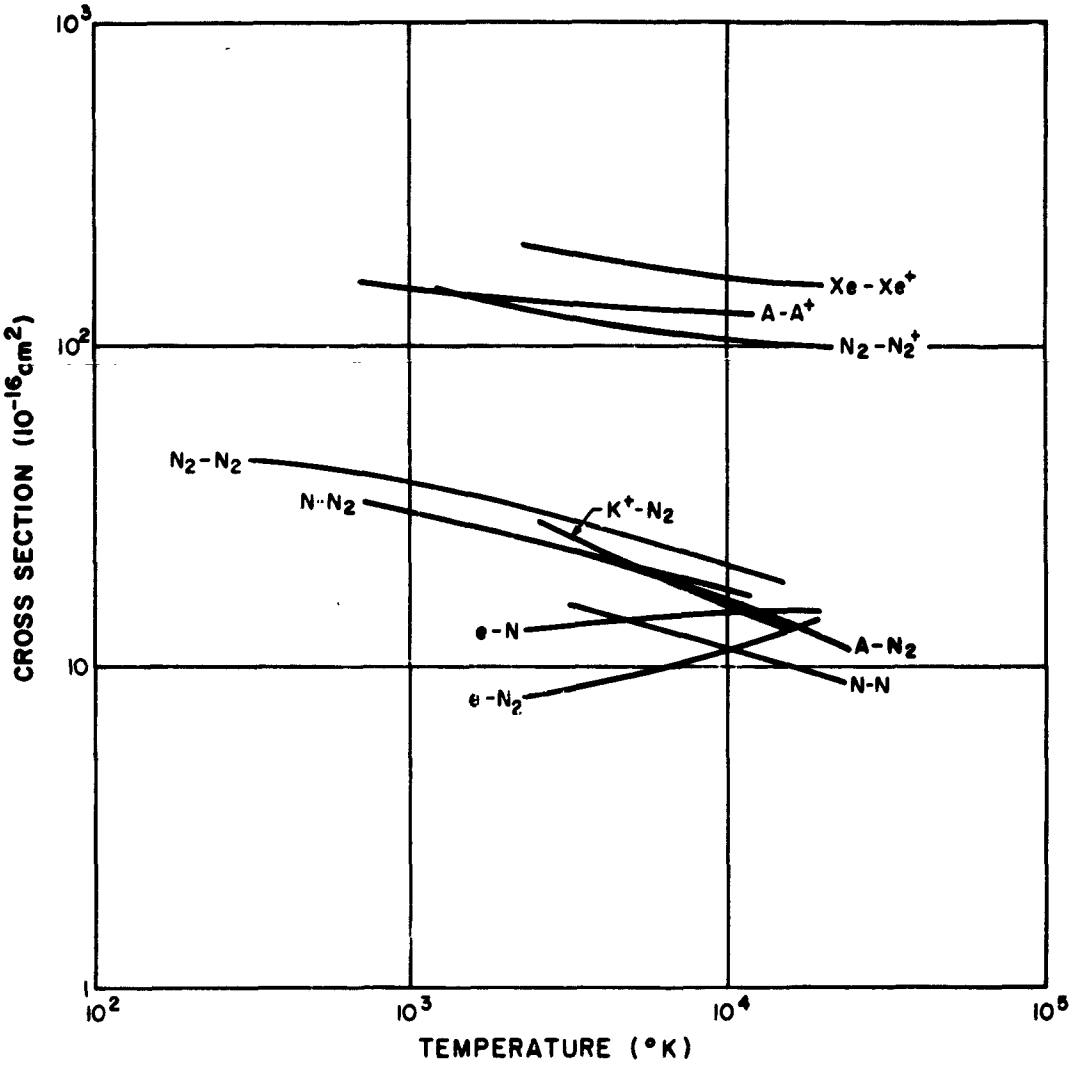

Fig. 3 - A summary of average elastic collision cross-sections as a function of gas temperature. For references to the sources see Fig. 4 of Ref. 10.

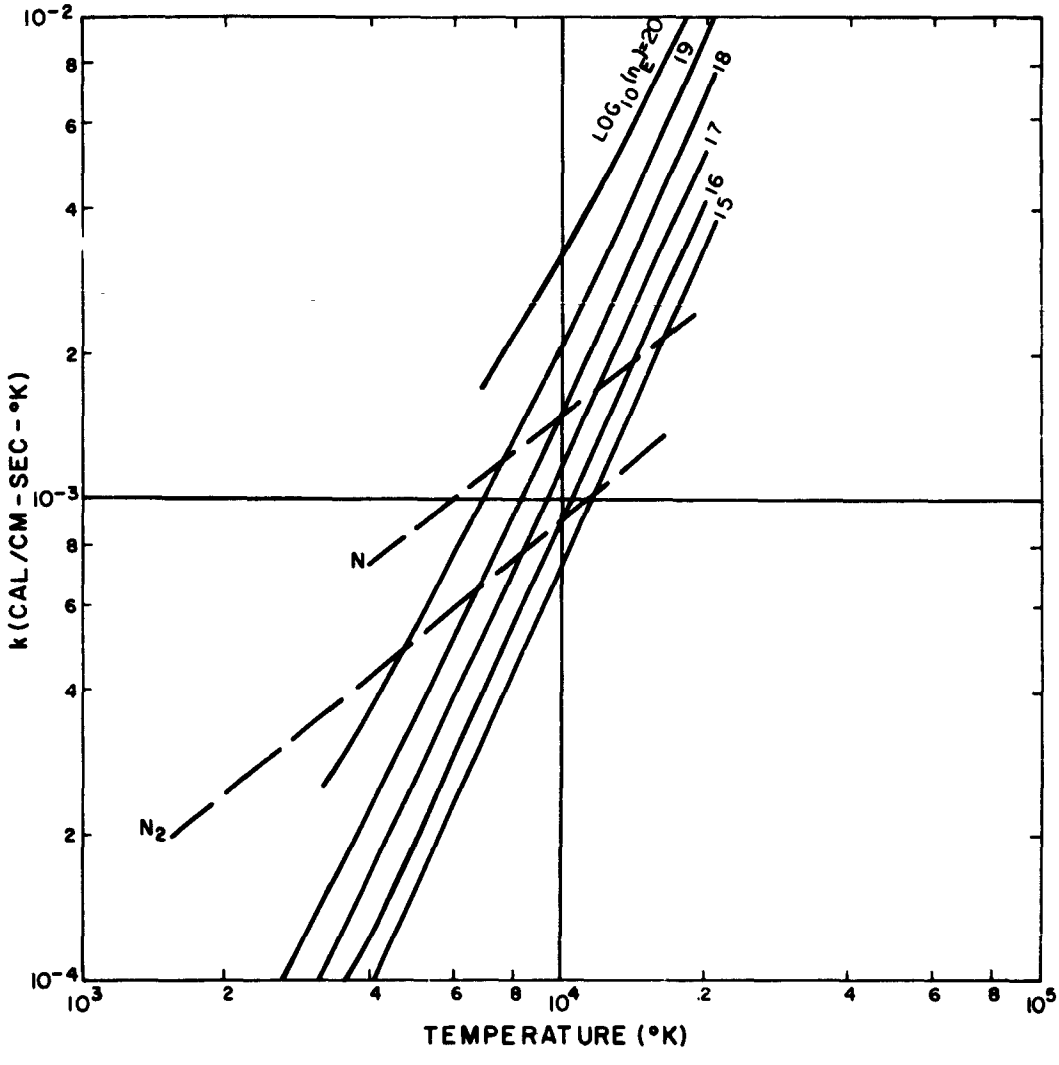

Fig. 4 - The frozen thermal conductivity of a singly ionized gas as a function of gas temperature and electron number density n_E in particles per cubic centimeter. The thermal conductivity of N and N_2 (Ref. 22) are shown for comparison.

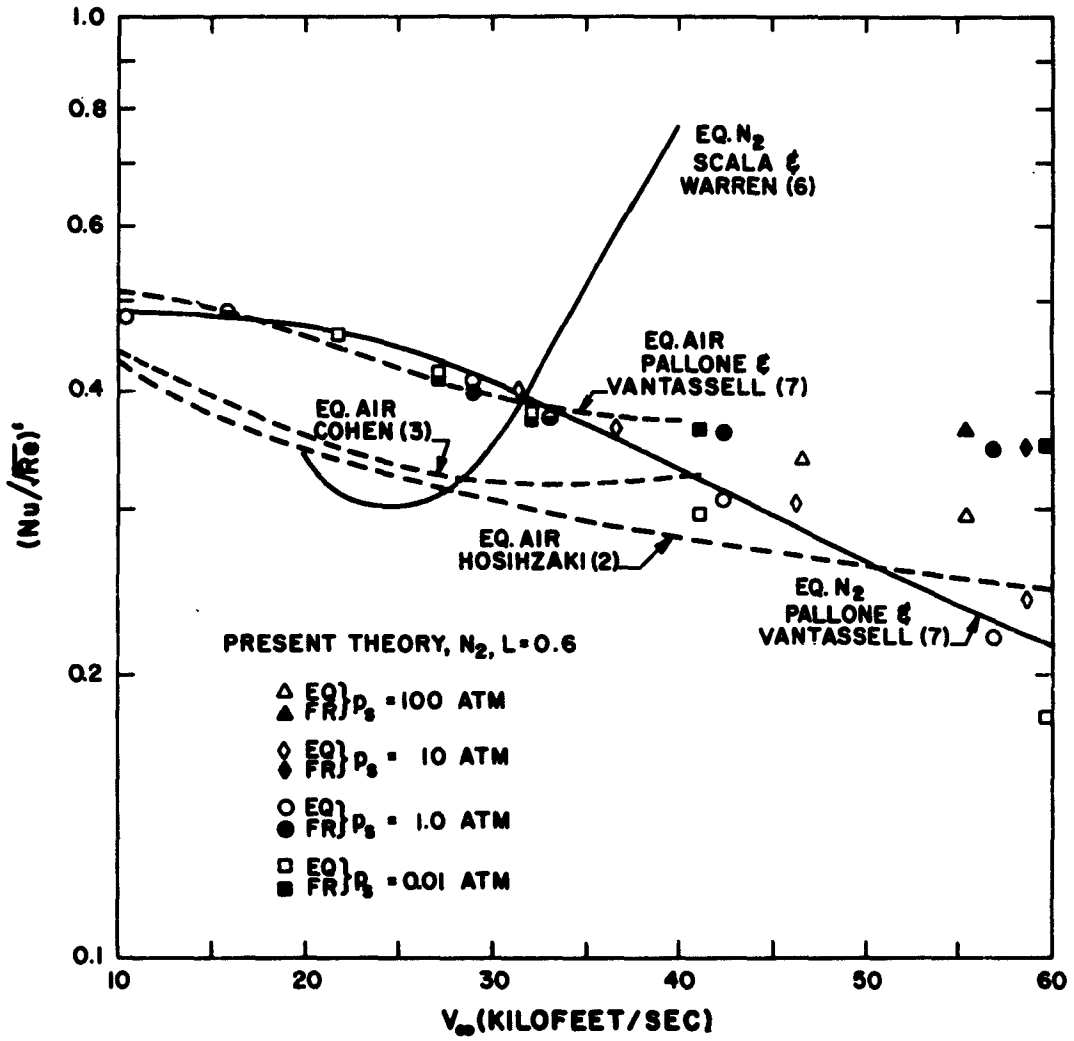

Fig. 5 - Comparison of calculations for stagnation-point heat transfer in partially ionized air and nitrogen.

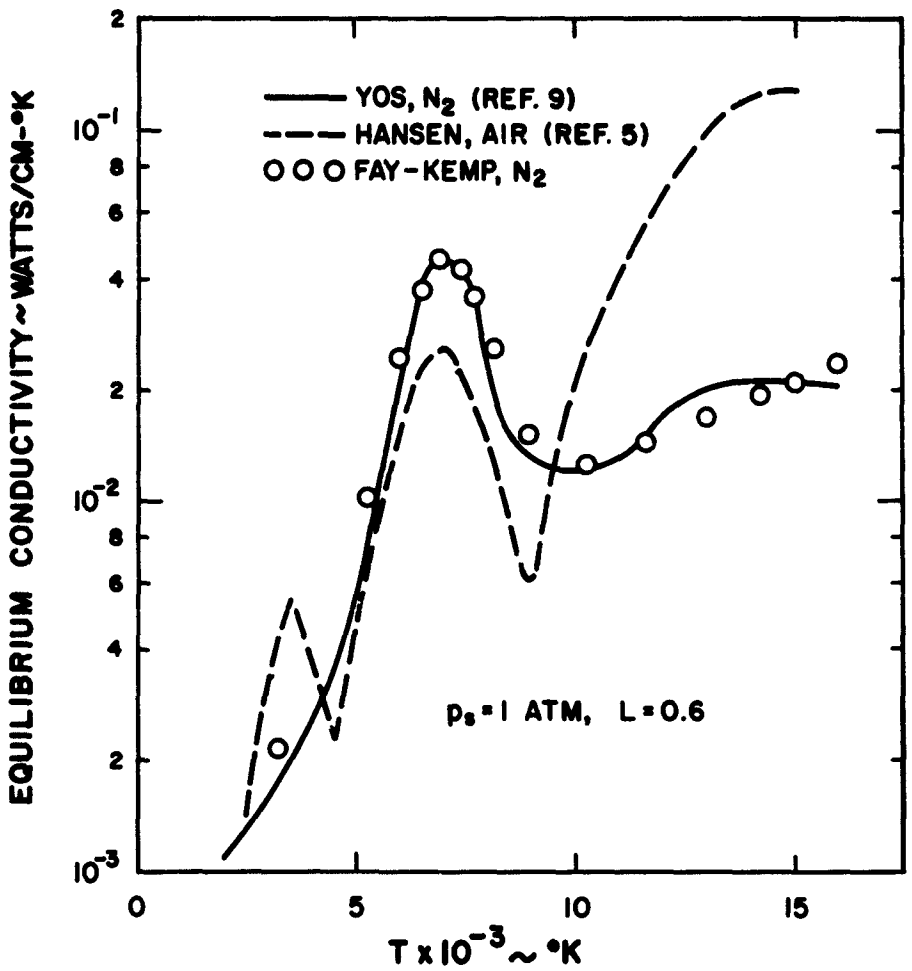

Fig. 6 - Comparison of equilibrium thermal conductivity used in several heat transfer calculations.

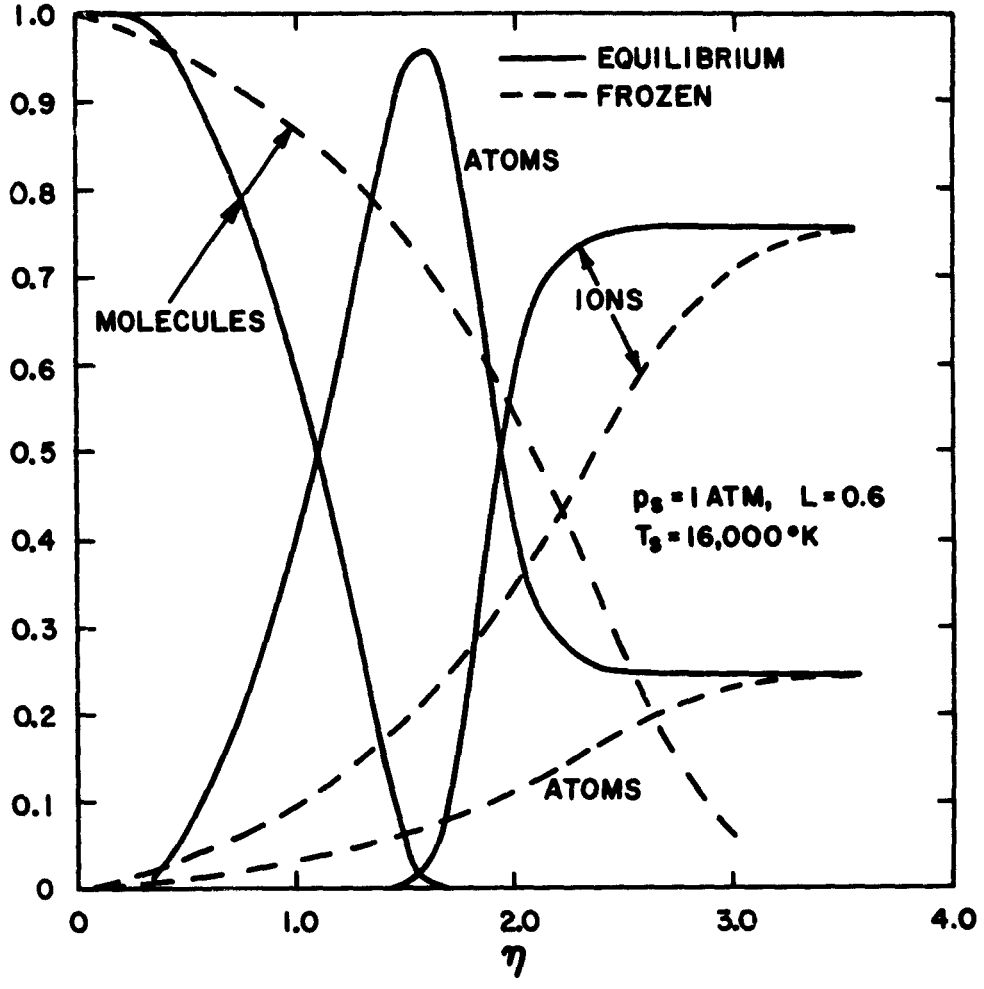

Fig. 7 - Species mass fraction distributions for p_s = 1 atm, L = 0.6, and T_s = 16,000°K.

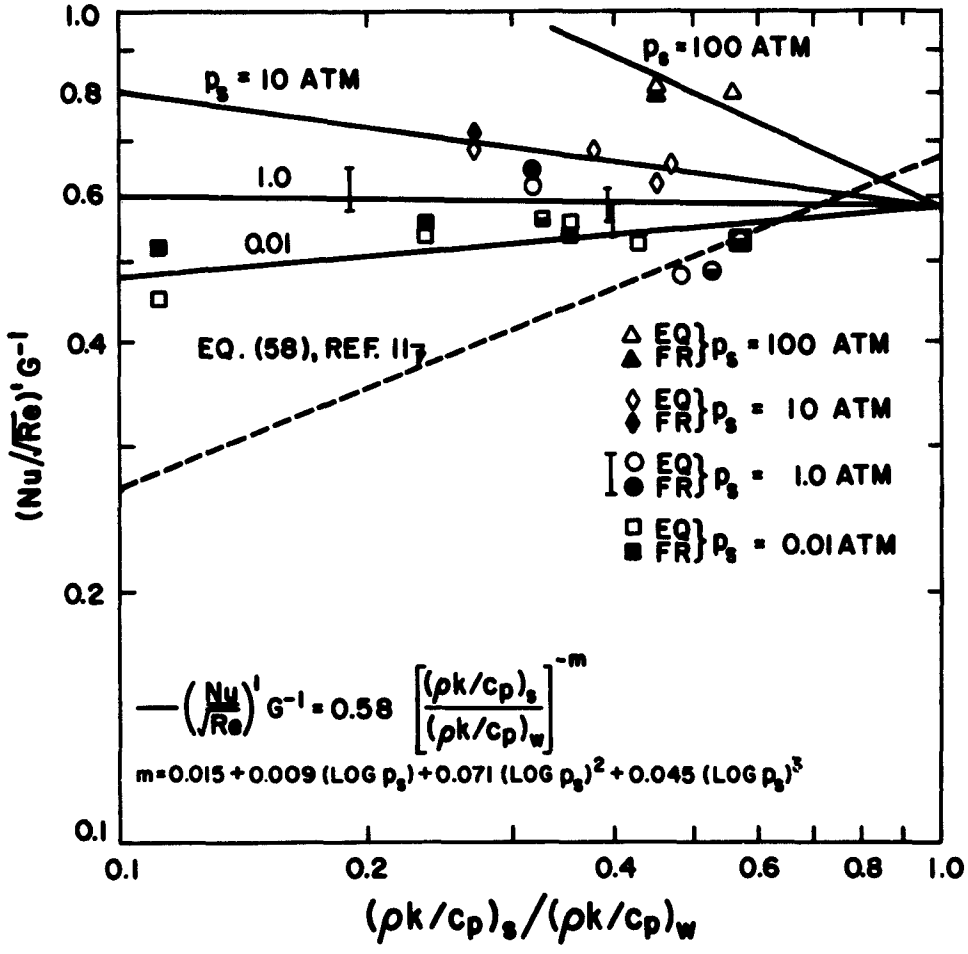

Fig. 8 - Correlation of heat transfer parameter in terms of transport properties. The quantity G is defined in Eq. (6. 3b).

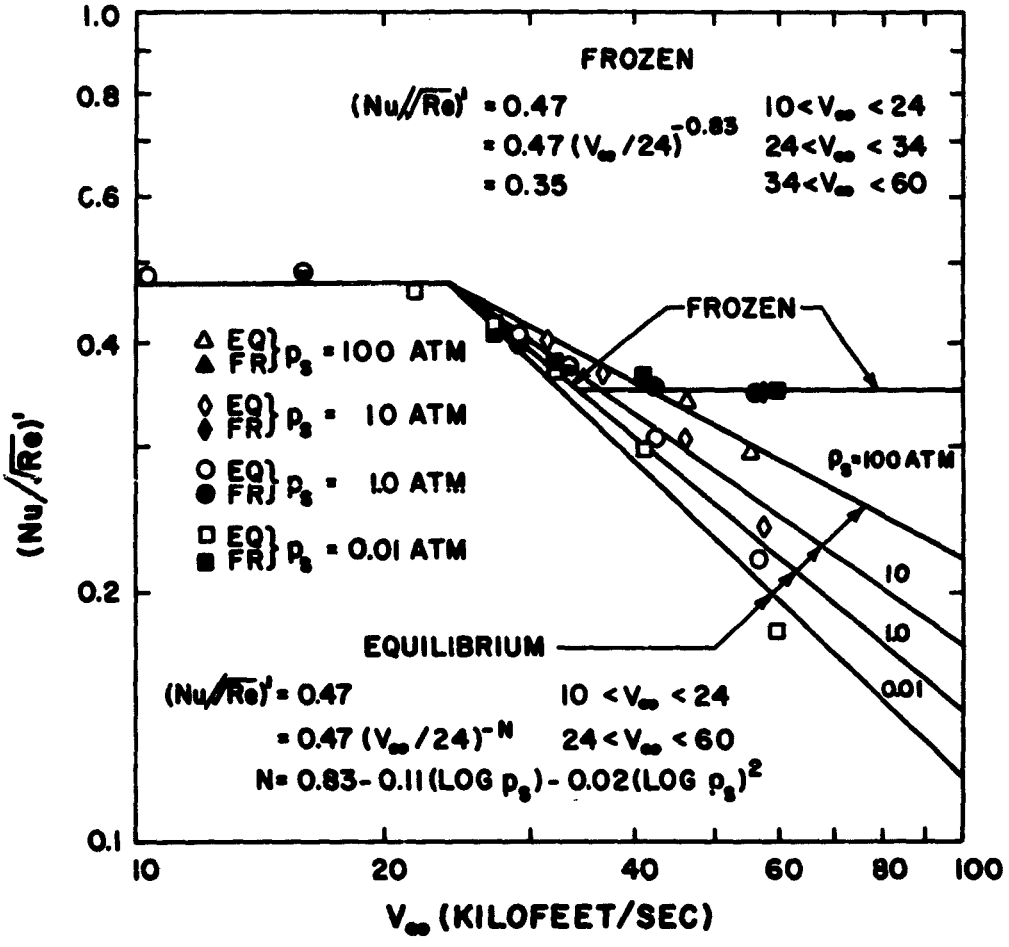

Fig. 9 - Correlation of heat transfer parameter in terms of flight velocity for L = 0.6.

Avco - Everett Research Laboratory, Everett, Massachusetts
THEORY OF STAGNATION POINT HEAT TRANSFER IN A PARTIALLY IONIZED DIATOMIC GAS, by James A. Fay and Nelson H. Kemp. April 1963. 60 p. incl. illus. (Avco - Everett Research Report 144; BSD - TDR - 62 - 347)
(Contract AF 04(694) - 33)

Unclassified report

Stagnation - point heat transfer in a partially ionized diatomic gas is considered. The concept of frozen thermal conductivity is used, and a simplified "binary diffusion" model of the gas is proposed. In this model the charge - exchange cross - section for atom - ion collisions is taken to be infinite so there is no relative diffusion of the atoms and the ion - electron pairs. This permits the diffusion effects to be dealt with as if there were only two components, molecules and atom - ion - electron particles, and thus greatly simplifies the calculations. However, the thermodynamic and transport properties are evaluated

(over)

UNCLASSIFIED

1. Heat transfer.
2. Gases, diatomic - Heat transfer.
3. Gases, ionized - Heat transfer.
4. Re - entry physics
I. Titie.
II. Fay, J. A.
III. Kemp, N. H.
IV. Avco - Everett Research Report 144.
V. AFBSD - TDR - 62 - 347.
VI. Contract AF 04(694) - 33.

UNCLASSIFIED

Avco - Everett Research Laboratory, Everett, Massachusetts
THEORY OF STAGNATION POINT HEAT TRANSFER IN A PARTIALLY IONIZED DIATOMIC GAS, by James A. Fay and Nelson H. Kemp. April 1963. 60 p. incl. illus. (Avco - Everett Research Report 144; BSD - TDR - 62 - 347)
(Contract AF 04(694) - 33)

Unclassified report

Stagnation - point heat transfer in a partially ionized diatomic gas is considered. The concept of frozen thermal conductivity is used, and a simplified "binary diffusion" model of the gas is proposed. In this model the charge - exchange cross - section for atom - ion collisions is taken to be infinite so there is no relative diffusion of the atoms and the ion - electron pairs. This permits the diffusion effects to be dealt with as if there were only two components, molecules and atom - ion - electron particles, and thus greatly simplifies the calculations. However, the thermodynamic and transport properties are evaluated

(over)

UNCLASSIFIED

1. Heat transfer.
2. Gases, diatomic - Heat transfer.
3. Gases, ionized - Heat transfer.
4. Re - entry physics.
I. Title.
II. Fay, J. A.
III. Kemp, N. H.
IV. Avco - Everett Research Report 144.
V. AFBSD - TDR - 62 - 347.
VI. Contract AF 04(694) - 33.

UNCLASSIFIED

using all four components, molecules, atoms, ions, and electrons. With this model, calculations are made for both frozen and equilibrium boundary layers in nitrogen up to about 60,000 ft/sec, and arguments are presented for applying the results to air. The results show the equilibrium heat transfer rate to be progressively smaller than the frozen rate as the velocity increases above 30,000 ft/sec, the ratio reaching 2/3 at 50,000 ft/sec. Simple correlation formulas for the results are given.

UNCLASSIFIED

UNCLASSIFIED